covalently bonded. The isotropic thermal parameters for the hydrogens of the bridging hydroxy groups refined to final values of 5 (1) and 8 (1) Å^2 for [**3**][PF_6] and 2 (1) and 3 (1) Å^2 for [**4**][PF_6]$_2$. All subsequent structure factor calculations for both compounds employed a least-squares refinable extinction correction.[17]

The final cycles of counter-weighted[18] cascade block-diagonal least-squares refinement, which employed anisotopic thermal parameters for all non-hydrogen atoms and isotropic thermal parameters for all hydrogen atoms, gave $R_1 = 0.047$ and R_2 (weighted, based on F)[16] = 0.046 for 5205 independent reflections of [**3**][PF_6] having $2\theta_{\text{Mo K}\alpha} < 55°$ and $I > 3\sigma(I)$. Similar refinement cycles for [**4**][PF_6]$_2$ gave $R_1 = 0.050$ and $R_2 = 0.049$ for 5269 independent reflections having $2\theta_{\text{Mo K}\alpha} < 50.7°$ and $I > 3\sigma(I)$.

All structure factor calculations for both compounds employed recent tabulations of atomic form factors[13b] and anomalous dispersion corrections[13c] to the scattering factors of the Co, Cl, P, and F atoms. All calculations were performed on a Data General Eclipse S-200 or S-230 computer equipped with 256K of 16-bit words, a floating point processor for 32- and 64-bit arithmetic, and versions of the Nicolet EXTL and SHELXTL interactive crystallographic software packages as modified at the Crystalytics Co.

Registry No. [**3**][PF_6]·$2CH_2Cl_2$, 113219-41-3; [**4**][PF_6]$_2$·CH_2Cl_2·H_2O, 113249-30-2; [**5**][PF_6], 98481-30-2; [**5**][OAc], 113219-42-4; [**6**][PF_6], 98509-07-0; $Co(OAc)_2$, 71-48-7; [$(py)_3Co_3O(CH_3CH_2CO_2)_6$][$PF_6$], 113249-32-4; AcO_2H, 79-21-0.

Supplementary Material Available: For [$(py)_4Co_2(OAc)_3(OH)_2$][PF_6]·$2CH_2Cl_2$, [**3**][PF_6]·CH_2Cl_2, the crystal structure report, Table SI (anisotropic thermal parameters), Table SIII (fractional atomic coordinates for hydrogen atoms), Table SV (bond lengths and bond angles for anion and solvent non-hydrogen atoms), and Figures S1 and S2 (ORTEP drawings of anion and solvent molecules) and for [$(py)_5Co_3O(OAc)_3(OH)_2$][PF_6]$_2$·CH_2Cl_2·H_2O, [**4**][PF_6]$_2$·CH_2Cl_2·H_2O, the crystal structure report, Table SII (anisotropic thermal parameters), Table SIV (fractional atomic coordinates for hydrogen atoms), Tables SVI and SVII (bond lengths and angles for anions and solvent non-hydrogen atoms), Figure S3 (ORTEP drawings of PF_6^- anions), and Figure S4 (ORTEP drawings of solvent molecules) (30 pages); listings of calculated and observed structure factor amplitudes for both compounds (46 pages). Ordering information is given on any current masthead page.

---

(17) Larson, A. C. *Acta Crystallogr.* **1967**, *23*, 664.
(18) For counter weights: $\sigma_F = \{[\sigma(F_o)]^2 + (p|F_o|)^2\}^{1/2}$ where the "ignorance factor", p, has the value of 0.01 in this case.

Contribution from the Laboratoire de Chimie de Coordination, Associé au CNRS (UA 416), and Laboratoire de Cristallochimie et de Chimie Structurale, Associé au CNRS (UA 424), Université Louis Pasteur, F-67070 Strasbourg Cédex, France, and Laboratoire de Cristallochimie, Associé au CNRS (UA 254), Université de Rennes I, F-35042 Rennes Cédex, France

Tri- and Tetranuclear Palladium-Cobalt Clusters Containing Bridging $Ph_2PCH_2PPh_2$ (dppm) Ligands. Crystal Structures of [$Pd_2Co_2(\mu_3\text{-}CO)_2(CO)_5(\mu\text{-dppm})_2$] and [$Pd_2Co(\mu_3\text{-}CO)_2(CO)_2(\mu\text{-dppm})_2$][$PF_6$]

Pierre Braunstein,[*,†] Claude de Méric de Bellefon,[†] Michel Ries,[†] Jean Fischer,[‡] Salah-Eddine Bouaoud,[§] and Daniel Grandjean[§]

Received April 7, 1987

The heterotetranuclear cluster [$Pd_2Co_2(CO)_7(dppm)_2$] (**1**) was synthesized in high yield by the reaction of [$Co(CO)_4$]$^-$ with [$Pd_2Cl_2(dppm)_2$] (dppm = μ-$Ph_2PCH_2PPh_2$), whereas the A-frame complexes [$Pd_2Cl_2(\mu\text{-}Y)(dppm)_2$] (Y = CO, CH_2) are much less reactive. The molecular structure of **1**·2.5THF has been determined by X-ray diffraction. Crystal data: triclinic, space group $P\bar{1}$ with $Z = 2$, $a = 18.417$ (8) Å, $b = 14.798$ (6) Å, $c = 13.855$ (6) Å, $\alpha = 113.61$ (2)°, $\beta = 107.50$ (2)°, $\gamma = 82.20$ (2)°, $V = 3299$ Å^3, $R = 0.055$, $R_w = 0.076$. This cluster contains a metalloligated triangular core of which two edges are bridged by the dppm ligands in such a way that the four P atoms and the four metal atoms are almost coplanar. The lability of the P→Pd bond of the precursor complex accounts for the easy formal insertion of the $Co(CO)_3$ fragment into this bond. A metal-exchange reaction can be thermally induced that transforms **1** into the triangular cluster [$PdCo_2(CO)_5(dppm)_2$]. The reaction of **1** with anionic nucleophiles X^- was found to regioselectively break the exocyclic Pd–Co bond, and it afforded the clusters [$Pd_2CoX(CO)_3(dppm)_2$] (X = Cl, Br, I, OH, SCN). The reversibility of this reaction was investigated, and the reaction leading to the halogeno clusters was best carried out in acetone, proceeding faster depending upon the nature of X^- ($I^- \approx Br^- \gg Cl^-$) and of the corresponding cation ($PPN^+ \gg K^+, Na^+$). Re-formation of the exocyclic Pd–Co bond was observed in Et_2O. The cationic cluster [$Pd_2Co(CO)_4(dppm)_2$]$^+$ was prepared by carbonylation of the halide-substituted Pd_2Co clusters in the presence of a halide abstractor. Its unique Pd-bound terminal CO ligand is very labile and can be reversibly and selectively replaced by a solvent molecule (acetone, THF, MeCN) depending upon CO partial pressure. The molecular structure of [$Pd_2Co(CO)_4(dppm)_2$][PF_6]·C_3H_6O (**7**·acetone) has been determined by X-ray diffraction. Crystal data: monoclinic, space group Cc with $Z = 4$, $a = 22.87$ (2) Å, $b = 14.198$ (4) Å, $c = 22.27$ (2) Å, $\beta = 122.35$ (5)°, $V = 6109$ Å^3, $R = 0.053$, $R_w = 0.069$. The structure of the cation may be considered as derived from that of **1** by the replacement of the terminally bound $Co(CO)_4$ unit by a carbonyl group. Spectroscopic IR and ^1H and $^{31}P\{^1H\}$ NMR data are discussed in relation with the structure and reactivity of these new clusters. The synthesis and chemistry of **1** are characterized by reactions formally taking place within the Pd_2P_4 plane. The bonding description of the clusters with a $Pd_2Co(dppm)_2$ core emphasizes their belonging to a new class of clusters where an anionic 18-electron metal carbonyl fragment is part of a closo structure.

Introduction

Bis(diphenylphosphino)methane (dppm), first synthesized by Issleib and Müller in 1959,[1] is presently playing a key role as a small-bite bidentate ligand in di- and polynuclear chemistry.[2,3] This ligand is remarkably versatile in its properties, allowing the stabilization of, e.g., dinuclear metal–metal-bonded complexes (A), A-frame complexes (B), double A-frame (C) complexes, or face-to-face eight-membered dimetallocycles $M_2(\mu\text{-dppm})_2$ (D), just to name examples where trans P–M–P arrangements are found.

[†] Laboratoire de Chimie de Coordination, Université Louis Pasteur.
[‡] Laboratoire de Cristallochimie et de Chimie Structurale, Université Louis Pasteur.
[§] Université de Rennes I.

(1) Issleib, K.; Müller, D.-W. *Chem. Ber.* **1959**, *92*, 3175.
(2) (a) Brown, M. P.; Fisher, J. R.; Franklin, S. J.; Puddephatt, R. J.; Thomson, M. A. In *Catalytic Aspects of Metal Phosphine Complexes*; Alyea, E. L., Meek, D. W., Eds.; Advances in Chemistry 196; American Chemical Society: Washington, DC, 1982; p 231. (b) Puddephatt, R. J. *Chem. Soc. Rev.* **1983**, *12*, 99 and references cited therein.
(3) (a) Balch, A. L. In *Catalytic Aspects of Metal Phosphine Complexes*; Alyea, E. L., Meek, D. W., Eds.; Advances in Chemistry 196; American Chemical Society: Washington, DC, 1982; p 243 and references cited therein. (b) Balch, A. L. In *Homogeneous Catalysis with Metal Phosphine Complexes*; Pignolet, L., Ed.; Plenum: New York, 1983; p 167.

0020-1669/88/1327-1327$01.50/0 © 1988 American Chemical Society

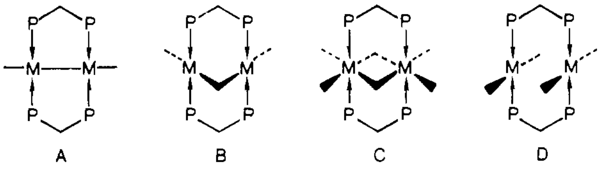

The metals most often involved in these structures are Rh,[4] Ir,[5] Pd,[3] and Pt,[2,6] frequently in the form of their halide complexes. Furthermore, dinuclear carbonyl complexes of, e.g., Mo,[7] Mn,[8] Re,[9] Fe,[10] and Co[11] containing the dppm ligand have also been investigated. A number of unique chemical features have been observed as a result of the proximity of the two metals in dppm complexes. These frequently involve metal–metal bond forming or bond breaking or electron-transfer reactions. Many of these complexes are able to coordinate (sometimes reversibly), in a bridging manner, atoms or small molecules such as H,[2,3,4d,6a,b,d,7,9b,12] S,[2a] SO_2,[2,3,13c] CO,[2,3,13c,14] RO^-,[15] RS^-,[2] CN^-,[8b] CS_2,[2,4a] CNR,[2,3,6f,16] C_2R_2,[2,3,5,13b] C_2R^-,[6g,17,18] N_2R^+,[2b,3b] and N_2CRR',[2b,4e,8c,11b] or unstable species such as CH_2.[2b,3b,10b,11b,13a] Unusual bonding modes for these ligands can result, which may be of relevance to their dynamic behavior[6b,c,8a,11c,19] and to stoichiometric or catalytic processes involving binuclear activation.[4b,6b,8a,10b,11d] Homogeneous catalysis with complexes having a $M_2(\mu\text{-dppm})_{2\text{ or }3}$ framework includes carbon–carbon multiple-bond hydrogenation,[20] alkene hydroformylation,[20c] alkyne cyclotrimerization,[21] the water gas shift reaction,[6a,20c,22] CO[23a] and CO_2[23a,24] hydrogenation, and NO and O_2 reduction by CO.[25] On the other hand, dppm is attracting interest as a stabilizing ligand in dinuclear metal-metal multiply bonded complexes.[2b,26] The very diverse chemistry of the ho-

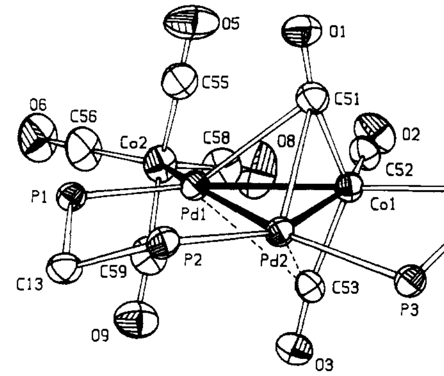

Figure 1. Perspective drawing of the molecular structure of $[Pd_2Co_2(CO)_7(dppm)_2]$ (**1**) illustrating the atom-numbering scheme. For clarity, the eight phenyl groups are not represented. Thermal ellipsoids enclose 50% of the electron density.

Scheme I

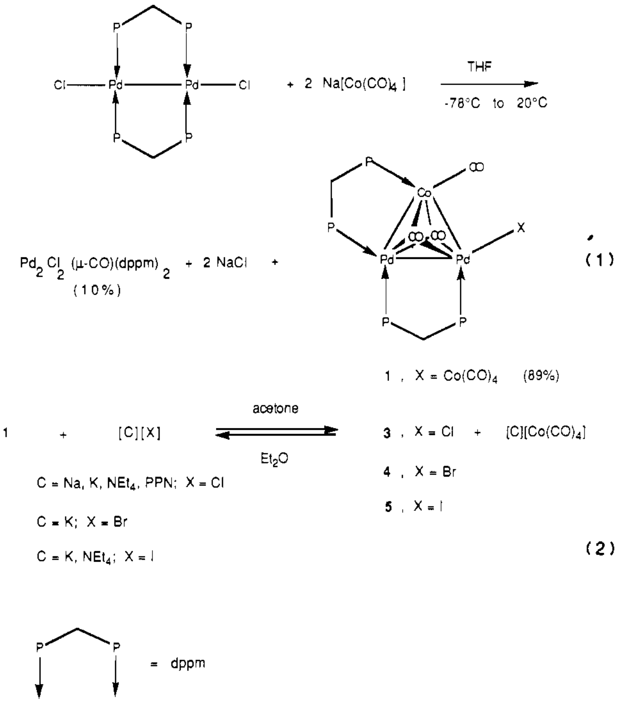

---

(4) For Rh complexes, see for example: (a) Cowie, M.; Dwight, S. K. *J. Organomet. Chem.* **1981**, *214*, 233. (b) Woodcock, C.; Eisenberg, R. *Organometallics* **1982**, *1*, 886. (c) Mague, J. T. *Inorg. Chem.* **1983**, *22*, 45. (d) Sutherland, B. R.; Cowie, M. *Inorg. Chem.* **1984**, *23*, 1290. (e) Woodcock, C.; Eisenberg, R. *Organometallics* **1985**, *4*, 4. (f) Ladd, J. A.; Olmstead, M. M.; Balch, A. L. *Inorg. Chem.* **1984**, *23*, 2318 and references cited therein.

(5) For Ir complexes, see for example: (a) Sutherland, B. R.; Cowie, M. *Organometallics* **1984**, *3*, 1869. (b) Mague, J. T.; Klein, C. L.; Majeste, R. J.; Stevens, E. D. *Organometallics* **1984**, *3*, 1860 and references cited therein.

(6) For Pt complexes, see for example: (a) Fisher, J. R.; Mills, A. J.; Sumner, S.; Brown, M. P.; Thomson, M. A.; Puddephatt, R. J.; Frew, A. A.; Manojlović-Muir, L.; Muir, K. W. *Organometallics* **1982**, *1*, 1421. (b) Puddephatt, R. J.; Azam, K. A.; Hill, R. H.; Brown, M. P.; Nelson, C. D.; Moulding, R. P.; Seddon, K. R.; Grossel, M. C. *J. Am. Chem. Soc.* **1983**, *105*, 5642. (c) Grossel, M. C.; Moulding, R. P.; Seddon, K. R. *J. Organomet. Chem.* **1983**, *247*, C32. (d) Hill, R. H.; Puddephatt, R. J. *J. Am. Chem. Soc.* **1983**, *105*, 5797. (e) Brown, M. P.; Yavari, A.; Manojlović-Muir, L.; Muir, K. W. *J. Organomet. Chem.* **1983**, *256*, C19. (f) Grundy, K. R.; Robertson, K. N. *Organometallics* **1983**, *2*, 1736. (g) Hutton, A. T.; Shebanzadeh, B.; Shaw, B. L. *J. Chem. Soc., Chem. Commun.* **1984**, 549. (h) Pringle, P. G.; Shaw, B. L. *J. Chem. Soc., Dalton Trans.* **1984**, 849. (i) Grossel, M. C.; Batson, J. R.; Moulding, R. P.; Seddon, K. R. *J. Organomet. Chem.* **1986**, *304*, 391 and references cited therein.

(7) For molybdenum carbonyl complexes, see for example: Darensbourg, M. Y.; El Mehdawi, R.; Delord, T. J.; Fronczek, F. R.; Watkins, S. F. *J. Am. Chem. Soc.* **1984**, *106*, 2583.

(8) For manganese carbonyl complexes, see for example: (a) Marsella, J. A.; Caulton, K. G. *Organometallics* **1982**, *1*, 274. (b) Aspinall, H. C.; Deeming, A. J.; Donovan-Mtunzi, S. *J. Chem. Soc., Dalton Trans.* **1983**, 2669. (c) Ferguson, G.; Laws, W. J.; Parvez, M.; Puddephatt, R. J. *Organometallics* **1983**, *2*, 276. (d) Aspinall, H. C.; Deeming, A. J. *J. Chem. Soc., Dalton Trans.* **1985**, 743 and references cited therein.

(9) For rhenium carbonyl complexes, see for example: (a) Prest, D. W.; Mays, M. J.; Raithby, P. R.; Orpen, A. G. *J. Chem. Soc., Dalton Trans.* **1982**, 737. (b) Prest, D. W.; Mays, M. J.; Raithby, P. R. *J. Chem. Soc., Dalton Trans.* **1982**, 2021. (c) Lee, K.-W.; Pennington, W. T.; Cordes, A. W.; Brown, T. L. *Organometallics* **1984**, *3*, 404 and references cited therein.

(10) For Fe complexes, see for example: (a) Cotton, F. A.; Troup, J. M. *J. Am. Chem. Soc.* **1974**, *96*, 4422. (b) Dawkins, G. M.; Green, M.; Orpen, A. G.; Stone, F. G. A. *J. Chem. Soc., Chem. Commun.* **1982**, 41. (c) Wright, M. E.; Mezza, T. M.; Nelson, G. O.; Armstrong, N. R.; Day, V. W.; Thompson, M. R. *Organometallics* **1983**, *2*, 1711 and references cited therein.

(11) For Co complexes, see for example: (a) Hanson, B. E.; Fanwick, P. E.; Mancini, J. S. *Inorg. Chem.* **1982**, *21*, 3811. (b) Laws, W. J.; Puddephatt, R. J. *J. Chem. Soc., Chem. Commun.* **1983**, 1020. (c) Hanson, B. E.; Mancini, J. C. *Organometallics* **1983**, *2*, 126. (d) Laws, W. J.; Puddephatt, R. J. *J. Chem. Soc., Chem. Commun.* **1984**, 116 and references cited therein.

(12) Woodcock, C.; Eisenberg, R. *Inorg. Chem.* **1984**, *23*, 4207.

(13) (a) McKeer, I. R.; Cowie, M. *Inorg. Chim. Acta* **1982**, *65*, L107. (b) Mague, J. T. *Inorg. Chem.* **1983**, *22*, 45. (c) Cowie, M.; Dickson, R. S.; Hames, B. W. *Organometallics* **1984**, *3*, 1879.

(14) Pringle, P. G.; Shaw, B. L. *J. Chem. Soc., Dalton Trans.* **1983**, 889.

(15) Deraniyagala, S. P.; Grundy, K. R. *Inorg. Chem.* **1985**, *24*, 50.

(16) DeLaet, D. L.; Powell, D. R.; Kubiak, C. P. *Organometallics* **1985**, *4*, 954.

(17) Blagg, A.; Hutton, A. T.; Pringle, P. G.; Shaw, B. L. *J. Chem. Soc., Dalton Trans.* **1984**, 1815.

(18) Cowie, M.; Loeb, S. J. *Organometallics* **1985**, *4*, 852.

(19) (a) Muralidharan, S.; Espenson, J. H. *J. Am. Chem. Soc.* **1984**, *106*, 8104. (b) Blau, R. J.; Espenson, J. H. *Ibid.* **1986**, *108*, 1962.

(20) (a) Stern, E. W.; Maples, P. K. *J. Catal.* **1972**, *27*, 120. (b) Kubiak, C. P.; Woodcock, C.; Eisenberg, R. *Inorg. Chem.* **1980**, *19*, 2733. (c) Kubiak, C. P.; Woodcock, C.; Eisenberg, R. *Inorg. Chem.* **1982**, *21*, 2119. (d) Sanger, A. R. *Can. J. Chem.* **1982**, *60*, 1363.

(21) Lee, C.-L.; Hunt, C. T.; Balch, A. L. *Inorg. Chem.* **1981**, *20*, 2498.

(22) Frew, A. A.; Hill, R. H.; Manojlović-Muir, L.; Muir, K. W.; Puddephatt, R. J. *J. Chem. Soc., Chem. Commun.* **1982**, 198.

(23) (a) Hoskins, B. F.; Steen, R. J.; Turney, T. W. *Inorg. Chim. Acta* **1983**, *77*, L69. (b) Hoskins, B. F.; Steen, R. J.; Turney, T. W. *J. Chem. Soc., Dalton Trans.* **1984**, 1831.

(24) Denise, B.; Sneeden, R. P. A. *J. Organomet. Chem.* **1981**, *221*, 111.

(25) Chin, C. S.; Sennett, M. S.; Wier, P. J.; Vaska, L. *Inorg. Chim. Acta* **1978**, *31*, L443.

mometallic dppm complexes has been reviewed recently by Puddephatt[2] and Balch[3] and has given rise to theoretical studies.[27]

Because of the rich potential both of dppm as a ligand and of mixed-metal clusters in general,[28,29] we have attempted to combine these two facets of chemistry by studying the synthesis, structural characterization, and reactivity of mixed-metal clusters containing the dppm ligand. Such studies are also relevant to the important question of selective metal–ligand interactions in mixed-metal clusters[29] and have already led, e.g., to the stabilization of palladium–iron clusters used as molecular precursors of new, selective heterogeneous carbonylation catalysts.[30] The first heterometallic dppm complex appears to be the dinuclear $[CpNi(\mu\text{-}SPh)(\mu\text{-}dppm)Mo(CO)_4]$ (Cp = $\eta\text{-}C_5H_5$),[31] whereas $[PdPtCl_2(\mu\text{-}dppm)_2]$[14] was the first heterodinuclear dppm complex with a metal–metal bond.

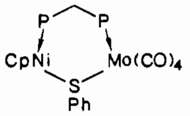

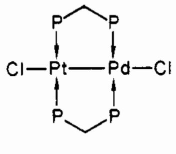

Since our preliminary communications on the synthesis and first structural characterization of dppm mixed-metal clusters, of core composition $Pd_2Co_2(\mu\text{-}dppm)_2$ and $Pd_2Mn_2(\mu\text{-}dppm)_2$,[32,33a] as well as of a bimetallic $PdMn(\mu\text{-}dppm)_2$ complex,[33a] studies carried out principally in Shaw's group have led to the synthesis of a large number of heterodinuclear complexes of the type $MM'(\mu\text{-}dppm)_2$.[17,23,34–36] However, the number of mixed-metal clusters containing dppm ligands has remained rather limited,[37a–c,46] and we report here the results of our investigations in this area. The systems presented here with M^2 = Co belong to a new class of clusters characterized by an almost planar heterotriangulo bis[bis(diphenylphosphino)methane] framework:

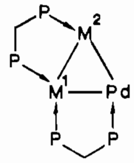

M^1 = Pd, Pt
M^2 = Mo,[32] W,[32] Mn,[33] Fe,[30,33b,40] Co[32,41]

Previous reactivity studies on bimetallic $(\mu\text{-}dppm)_2$ systems have emphasized the robustness of the metal–phosphorus bonds in the M_2P_4 core and shown that much of the chemistry occurring on or between the metal centers was actually taking place in a plane *perpendicular* to the M_2P_4 plane. Other studies have pointed to the conformational flexibility of the M_2P_4 core structure, without rupture of the metal–phosphorus bonds.[47] Our findings, in contrast, indicate that another type of reactivity can be observed with these molecules, which formally takes place *within* the M_2P_4 plane, owing to the lability of the metal–phosphorus bond.

Results

Synthesis of the Tetranuclear Cluster $[Pd_2Co_2(CO)_7(dppm)_2]$ (1). The reaction of 2 equiv of $Na[Co(CO)_4]$ with $[Pd_2Cl_2(dppm)_2]$ (in the following, dppm = $\mu\text{-}Ph_2PCH_2PPh_2$) was monitored by IR spectroscopy in the ν(CO) region and was stopped after stabilization of the new absorption bands. It afforded the deep green Pd_2Co_2 cluster **1** in high yield (eq 1 in Scheme I), accompanied by a small amount of the CO-insertion product $[Pd_2Cl_2(\mu\text{-}CO)(dppm)_2]$, resulting from the ready uptake by the precursor complex of the liberated CO.[48]

The solid-state structure of **1** has been determined by a single-crystal X-ray analysis (vide infra) and is shown in Figures 1 and 3.[83] The ^1H NMR spectrum of **1** shows two groups of CH_2 resonances, consistent with the structure of the complex. the $^{31}P\{^1H\}$ NMR spectrum reveals four groups of signals assigned to the four inequivalent phosphorus atoms. The low-field resonance is distinctively quadrupole broadened and is attributed to the phosphorus atom coordinated to Co(1). The assignment of the ^1H and $^{31}P\{^1H\}$ NMR resonances of the clusters described in this work was made by comparison with a family of related molecules and is discussed in the following paper.[49]

In order to determine whether $[Pd_2Cl_2(\mu\text{-}CO)(dppm)_2]$ could be an intermediate in the synthesis of **1** and to compare its reactivity with that of $[Pd_2Cl_2(dppm)_2]$, it was reacted with 2 equiv of $Na[Co(CO)_4]$. Complex **1** was again obtained, but the reaction required a higher temperature (20 °C) and a longer time (4 days) and afforded lower yields than when starting from $[Pd_2Cl_2(dppm)_2]$ (see Experimental Section). When the reaction of eq 1 was carried out with an *excess* of $[Co(CO)_4]^-$ (under the same experimental conditions as before), $[Pd_2Cl_2(\mu\text{-}CO)(dppm)_2]$ was still isolated at the end of the reaction. The isoelectronic A-frame complex $[Pd_2Cl_2(\mu\text{-}CH_2)(dppm)_2]$, prepared in high yield from $[Pd_2Cl_2(dppm)_2]$ and excess CH_2N_2, reacted with $Na[Co(CO)_4]$ in an even more sluggish manner, 90% of the starting material

---

(26) (a) Barder, T. J.; Cotton, F. A.; Lewis, D.; Schwotzer, W.; Tetrick, S. M.; Walton, R. A. *J. Am. Chem. Soc.* **1984**, *106*, 2882. (b) Campbell, F. L.; Cotton, F. A.; Powell, G. L. *Inorg. Chem.* **1984**, *23*, 4222. (c) Anderson, L. B.; Barder, T. J.; Walton, R. A. *Inorg. Chem.* **1985**, *24*, 1421.

(27) Hoffman, D. M.; Hoffmann, R. *Inorg. Chem.* **1981**, *20*, 3543.

(28) Gladfelter, W. L.; Geoffroy, G. L. *Adv. Organomet. Chem.* **1980**, *18*, 207.

(29) (a) Sappa, E.; Tiripicchio, A.; Braunstein, P. *Coord. Chem. Rev.* **1985**, *65*, 219. (b) Braunstein, P. *Nouv. J. Chim.* **1986**, *10*, 365.

(30) Braunstein, P.; Kervennal, J.; Richert, J.-L. *Angew. Chem., Int. Ed. Engl.* **1985**, *24*, 768.

(31) Sato, F.; Uemura, T.; Sato, M. *J. Organomet. Chem.* **1973**, *56*, C27.

(32) Braunstein, P.; Jud, J.-M.; Dusausoy, Y.; Fischer, J. *Organometallics* **1983**, *2*, 180.

(33) (a) Braunstein, P.; Jud, J.-M.; Fischer, J. *J. Chem. Soc., Chem. Commun.* **1983**, 5. (b) Braunstein, P.; de Méric de Bellefon, C.; Ries, M.; Fischer, J. *Organometallics* **1988**, *7*, 332–343.

(34) Carr, S. W.; Shaw, B. L. *J. Chem. Soc., Dalton Trans.* **1986**, 1815 and references cited therein.

(35) (a) Sabo, S.; Chaudret, B.; Gervais, D. *J. Organomet. Chem.* **1983**, *258*, C19. (b) Chaudret, B.; Delavaux, B.; Poilblanc, R. *Nouv. J. Chim.* **1983**, *7*, 679. (c) Delavaux, B.; Arliguie, T.; Chaudret, B.; Poilblanc, R. *Nouv. J. Chim.* **1986**, *10*, 619.

(36) (a) Cole-Hamilton, D. J.; Gregory, A. C.; Gooden, N. G.; Smith, G. *Polyhedron* **1982**, *1*, 97. (b) Uson, R.; Laguna, A.; Forniés, J.; Valenzuela, I.; Jones, P. G.; Sheldrick, G. M. *J. Organomet. Chem.* **1984**, *273*, 129.

(37) (a) Chetcuti, M. J.; Chetcuti, P. A. M.; Jeffery, J. C.; Mills, R. M.; Mitrprachachon, P.; Pickering, S. J.; Stone, F. G. A.; Woodward, P. *J. Chem. Soc., Dalton Trans.* **1982**, 699. (b) Busetto, L.; Jeffery, J. C.; Mills, R. M.; Stone, F. G. A.; Went, M. J.; Woodward, P. *J. Chem. Soc., Dalton Trans.* **1983**, 101. (c) Evans, D. G.; Howard, J. A. K.; Jeffery, J. C.; Lewis, D. B.; Lewis, G. E.; Grosse-Ophoff, M. J.; Parrott, M. J.; Stone, F. G. A. *J. Chem. Soc., Dalton Trans.* **1986**, 1723. (d) Abad, J. A.; Delgado, E.; Garcia, M. E.; Grosse-Ophoff, M. J.; Hart, I. J.; Jeffery, J. C.; Simmons, M. S.; Stone, F. G. A. *J. Chem. Soc., Dalton Trans.* **1987**, 41. (e) Farrugia, L. J.; Jeffery, J. C.; Marsden, C.; Sherwood, P.; Stone, F. G. A. *J. Chem. Soc., Dalton Trans.* **1987**, 51.

(38) Coleman, A. W.; Jones, D. F.; Dixneuf, P. H.; Brisson, C.; Bonnet, J. J.; Lavigne, G. *Inorg. Chem.* **1984**, *23*, 952.

(39) (a) Faraone, F.; Lo Schiavo, S.; Bruno, G.; Bombieri, G. *J. Chem. Soc., Chem. Commun.* **1984**, 6. (b) Bruno, G.; Lo Schiavo, S.; Piraino, P.; Faraone, F. *Organometallics* **1985**, *4*, 1098. (c) Bruno, G.; Lo Schiavo, S.; Piraino, P.; Faraone, F. *Ibid.* **1985**, *4*, 2091.

(40) Grossel, M. C.; Moulding, R. P.; Seddon, K. R. *J. Organomet. Chem.* **1983**, *253*, C50.

(41) Braunstein, P.; de Méric de Bellefon, C.; Ries, M. *J. Organomet. Chem.* **1984**, *262*, C14.

(42) Briant, C. E.; Hall, K. P.; Mingos, D. M. P. *J. Chem. Soc., Chem. Commun.* **1983**, 843.

(43) Ladd, J. A.; Hope, H.; Balch, A. L. *Organometallics* **1984**, *3*, 1838.

(44) Schroeder, N. C.; Richardson, J. W., Jr.; Wang, S.-L.; Jacobson, R. A.; Angelici, R. J. *Organometallics* **1985**, *4*, 1226.

(45) Bates, P. A.; Brown, S. S. D.; Dent, A. J.; Hursthouse, M. B.; Kitchen, G. F. M.; Orpen, A. G.; Salter, I. D.; Sik, V. *J. Chem. Soc., Chem. Commun.* **1986**, 600.

(46) Sharp, P. R. *Inorg. Chem.* **1986**, *25*, 4185.

(47) Ho, D. M.; Bau, R. *Inorg. Chem.* **1983**, *22*, 4073.

(48) Benner, L. S.; Balch, A. L. *J. Am. Chem. Soc.* **1978**, *100*, 6099.

(49) Braunstein, P.; de Méric de Bellefon, C.; Ries, M. *Inorg. Chem.*, following paper in this issue.

being recovered. The only product formed was **1** when this reaction was conducted in Et_2O whereas, under similar conditions (ambient temperature), no reaction occurred in THF.

Upon moderate heating (60–80 °C in toluene or THF), cluster **1** slowly transforms into the new species **2** (91% yield based on Co). Its $^{31}P\{^1H\}$ NMR spectrum clearly shows two types of inequivalent phosphorus atoms: one being coordinated to a Co atom and the other to a Pd atom. On the basis of spectroscopic and analytical data, the proposed structure for **2** is that of a triangular cluster with two dppm ligands spanning the PdCo bonds and a triply semibridging CO ligand. The same species was formed during the reaction of $[Pd_2Cl_2(\mu\text{-}CH_2)dppm)_2]$ with $Na[Co(CO)_4]$ in *refluxing* THF and probably resulted from the transformation upon heating of **1** already formed. A metal-exchange reaction is therefore thermally induced between the exocyclic cobalt atom of **1** and a palladium atom, which is expelled from the triangular core. No other Pd-containing complex could be detected during the transformation of **1** into **2**.

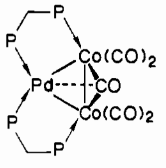

2

Reaction of 1 with Anionic Nucleophiles: Synthesis of the Trinuclear Clusters $[Pd_2CoX(CO)_3(dppm)_2]$ (X = Cl, 3; Br, 4; I, 5). The reactions of **1** with halide anions were investigated in order to determine the site selectivity of these reagents and to obtain functionalized clusters (see eq 2 in Scheme I). In general, the reactions were accompanied by a color change from green to red-brown. Shifting the position of the equilibrium of eq 2 to the right was achieved by working in appropriate solvents (e.g., acetone, THF). Note that in CH_2Cl_2 the reaction could be performed by using soluble iodides (e.g., NEt_4I). The forward reaction proceeded faster depending upon the nature of $[C]^+$ ($PPN^+ \gg K^+, Na^+$) and X^- ($I^- \approx Br^- \gg Cl^-$). No reaction occurred with NaF, even in acetone. In systems containing K^+ or Na^+, the equilibrium of eq 2 could be shifted to the left upon addition of a nonpolar solvent (e.g., pentane, *n*-hexane, or Et_2O). This shift was also observed when an acetone solution of **1** and KI (or of **5** and $K[Co(CO)_4]$) was evaporated to dryness. Therefore, the best way to isolate clusters **3**–**5** is to prevent nucleophilic attack of $[Co(CO)_4]^-$ on the Pd–X bond. This is achieved by using either a large associated cation (e.g., PPN^+), or a small cation (e.g., Na^+, K^+) in a biphasic medium (water/hexane). In these reactions, the use of Et_2O is precluded by the enhanced reactivity of $[Co(CO)_4]^-$ associated with Na^+ or K^+ in this medium. We also noticed that **1** partially transformed into **3** during the recording of a $^{31}P\{^1H\}$ NMR spectrum in $CDCl_3$. The reaction of **1** with KOH was accompanied by an immediate color change from dark green to deep violet, but all attempts to isolate the compound in the solid state led to the reformation of **1**. Reaction of **1** with NaH was very slow, and although IR spectroscopy showed the liberation of $[Co(CO)_4]^-$, no product could be isolated and characterized without decomposition occurring. Similarly, the reaction of **1** or **5** with $NaBH_4$ in THF led to decomposition. The iodide ligand of **5** may be readily exchanged by metathesis with potassium thiocyanate in acetone, affording the deep red cluster $[Pd_2Co(SCN)(CO)_3(dppm)_2]$ (**6**). The ambidentate nature of the thiocyanate ligand, which may bind in a linear fashion through the nitrogen atom or in a bent fashion through the sulfur atom, is well recognized. The $\nu(CN)$ value found for **6**, both in the solid state (2092 cm^{-1}) and in toluene solution (2094 cm^{-1}), is characteristic of a S-bound thiocyanate. This coordination mode, favored by a soft Pd metal center, is also found in the mixed-metal complex $[PdMn(SCN)(CO)_3(dppm)_2]$[23] and in the binuclear palladium complex $[Pd_2(SCN)_2(dppm)_2]$.[48] This latter presents a linkage isomerism (N bound) that is not observed by IR or NMR spectroscopy for **6** in solution. Replacement of the iodide ligand in **5** by Cl^- or F^- cannot be performed in acetone, even in the presence of an excess of NaF or NaCl.

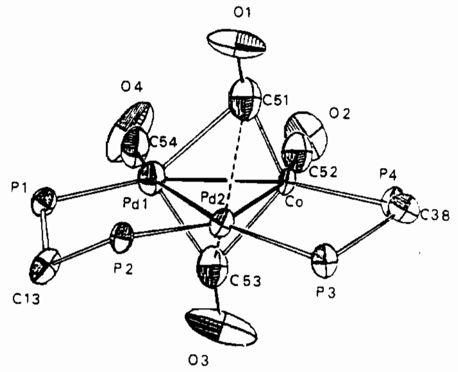

Figure 2. Perspective drawing of the $[Pd_2Co(CO)_4(dppm)_2]^+$ cation in **7** illustrating the atom-numbering scheme. For clarity, the eight phenyl groups are not represented. Thermal ellipsoids enclose 50% of the electron density.

Scheme II

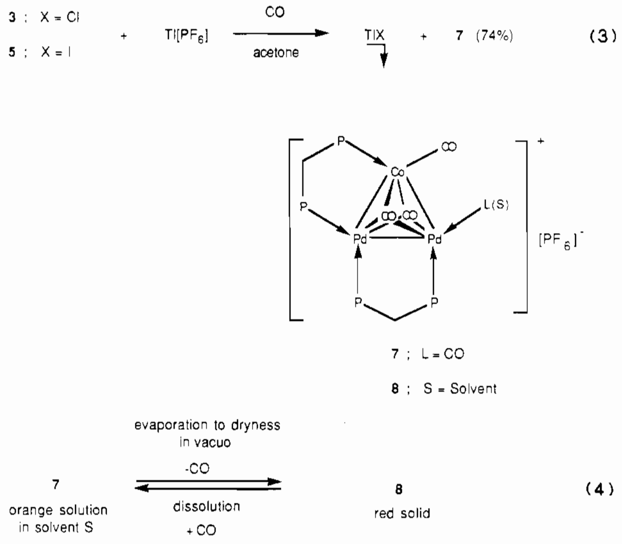

Clusters **3**–**6** present ^1H and $^{31}P\{^1H\}$ NMR patterns similar to those of **1**. The IR absorptions due to the coordinated $Co(CO)_4$ fragment of **1** are absent in **3**–**6**, thus facilitating their assignment (Figure 4[83]).

Carbonylation of 3 and 5: Synthesis of $[Pd_2Co(CO)_4(dppm)_2][PF_6]$ (7). Clusters **1**–**5** in THF did not react with CO at atmospheric pressure, nor did **5** in MeOH. However, the reaction of **3** or **5** with CO in the presence of $Tl[PF_6]$ led to an immediate lightening of the color of the solution to orange-red, and the trinuclear cationic cluster $[Pd_2Co(CO)_4(dppm)_2][PF_6]$ (**7**) was isolated in good yield (eq 3 in Scheme II). This complex presents ^1H and $^{31}P\{^1H\}$ NMR spectral patterns similar to those of its precursors. In contrast, its IR spectrum exhibits a new $\nu(CO)$ band at 2072 cm^{-1} (KBr), assigned to the terminal Pd-bound CO ligand (Figure 4[83]). It is noteworthy that this CO ligand was not displaced by Br^- when a KBr pellet was prepared (the intensity of the $\nu(CO)$ absorption was stable with time) in contrast to the solution behavior (see below). The solid-state structure of **7** was determined by a single-crystal X-ray diffraction analysis (vide infra) and is shown in Figure 2.

Reversible CO-Uptake Experiments. When an acetone, THF, MeCN, or CH_2Cl_2 solution of **7** was evaporated to dryness in vacuo, the IR spectrum (recorded in THF) of the red solid showed that the strong absorption band at 2078 cm^{-1} had almost disappeared. The solvento complexes **8** have a structure like **1** or **7**, except with a solvent molecule replacing $Co(CO)_4^-$ or CO, respectively. Bubbling CO through any of these red solutions restored immediately the original orange-red color and caused complete reappearance of the highest carbonyl absorption band

Table I. Selected Interatomic Distances and Angles in **1**·$2.5C_4H_8O$ and **7**·C_3H_6O

Bond Lengths (Å)[a]

bond[b]	**1**·$2.5C_4H_8O$	**7**·C_3H_6O
Pd(1)–Pd(2)	2.5861 (7)	2.559 (1)
Pd(1)–Co(1)	2.612 (1)	2.620 (2)
Pd(1)–Co(2)	2.728 (1)	
Pd(2)–Co(1)	2.512 (1)	2.551 (1)
Pd(1)–P(1)	2.270 (3)	2.283 (3)
Pd(2)–P(2)	2.274 (2)	2.289 (3)
Pd(2)–P(3)	2.295 (2)	2.257 (3)
Co(1)–P(4)	2.202 (2)	2.211 (3)
Co(1)–C(51)	1.785 (9)	1.67 (7)
Co(1)–C(52)	1.781 (9)	1.80 (2)
Co(1)–C(53)	1.801 (9)	2.08 (4)
Pd(1)–C(51)	2.536 (8)	2.36 (4)
Pd(2)–C(51)	2.488 (8)	2.47 (3)
Pd(1)–C(53)	2.598 (8)	2.21 (5)
Pd(2)–C(53)	2.626 (8)	2.47 (2)
Pd(1)–C(54)		1.91 (2)
Pd(1)–C(55)	2.52 (1)	
Pd(1)–C(59)	2.59 (1)	
Co(2)–C(55)	1.78 (1)	
Co(2)–C(56)	1.78 (1)	
Co(2)–C(58)	1.81 (1)	
Co(2)–C(59)	1.77 (1)	

Bond Angles (deg)[a]

angle[b]	**1**·$2.5C_4H_8O$	**7**·C_3H_6O
Pd(2)–Pd(1)–Co(1)	57.79 (3)	59.01 (4)
Pd(1)–Pd(2)–Co(1)	61.63 (3)	61.67 (4)
Pd(2)–Pd(1)–Co(2)	161.23 (4)	
Pd(2)–Pd(1)–P(1)	92.45 (5)	93.24 (8)
Pd(1)–Pd(2)–P(2)	97.58 (5)	96.79 (8)
Co(1)–Pd(2)–P(3)	95.44 (5)	97.86 (8)
Co(1)–C(51)–O(1)	167 (1)	167 (4)
Co(1)–C(53)–O(3)	170.6 (9)	142 (5)
Co(2)–C(55)–O(5)	168.4 (9)	
Co(2)–C(59)–O(9)	169.5 (8)	
Pd(2)–Co(1)–P(4)	96.17 (6)	94.59 (8)
P(2)–Pd(2)–P(3)	105.92 (6)	103.8 (1)
P(1)–Pd(1)–Co(2)	104.37 (6)	
P(1)–Pd(1)–C(54)		106.7 (5)
P(4)–Co(1)–C(51)	99.1 (3)	110.0 (1)
P(4)–Co(1)–C(52)	99.2 (3)	105.4 (5)
P(4)–Co(1)–C(53)	112.4 (2)	116.0 (2)
C(51)–Co(1)–C(52)	104.9 (4)	105.8 (9)
C(51)–Co(1)–C(53)	132.0 (4)	113.0 (2)
C(52)–Co(1)–C(53)	104.7 (4)	104.5 (7)
C(55)–Co(2)–C(56)	105.5 (5)	
C(55)–Co(2)–C(58)	106.0 (6)	
C(55)–Co(2)–C(59)	130.2 (4)	
C(56)–Co(2)–C(58)	106.3 (6)	
C(56)–Co(2)–C(59)	101.4 (5)	
C(58)–Co(2)–C(59)	105.5 (6)	

[a] Figures in parentheses are the estimated standard deviations in the last significant digits. [b] Atoms are labeled in agreement with Figures 1 and 2.

at 2078 cm^{-1}. This uptake of carbon monoxide is reversible (eq 4 in Scheme II), and many cycles of carbonylation–decarbonylation could be performed without noticeable decomposition in THF, acetone, or MeCN. Bubbling nitrogen or argon through a CH_2Cl_2 solution of **7** did not afford the decarbonylation product, whereas this occurred in acetone, THF, or MeCN after 0.5 h. Furthermore, this terminal Pd-bound CO can be readily displaced by anionic nucleophiles since an acetone solution of **7** immediately reacted with NaCl or KBr with formation of **3** and **4**, respectively.

Crystal Structures of $[Pd_2Co_2(CO)_7(dppm)_2]\cdot2.5C_4H_8O$ (1·2.5THF) and $[Pd_2Co(CO)_4(dppm)_2][PF_6]\cdot C_3H_6O$ (7·Me$_2$CO). The labeling schemes used in the description of these molecules on the ORTEP plots are given in Figures 1 and 2. Selected bond distances and angles for both clusters are given in Table I. Cluster **1** crystallizes with 2.5 molecules of THF whose disorder could not be resolved. The framework of this heterotetranuclear cluster consists of a triangular core ligated by a $Co(CO)_4$ fragment. The two dppm ligands bridge the Pd(1)–Pd(2) and Pd(2)–Co(1) edges in such a way that the four phosphorus atoms and the four metal atoms are almost coplanar, the maximum deviation from their mean plane being 0.494 (2) Å for P(2) (Table S-V[83]). This cluster belongs to the small class of the so-called "metalloligated" or "spiked-triangular" clusters, i.e., those that have a tetranuclear core consisting of a triangle with an equatorially or axially substituted pendant organometallic unit coordinated to it. Planar structures of this type are relatively rare in cluster chemistry, but examples are known with the core compositions Re_4,[50] Os_4,[51] Ru_4,[52] $CrReRh_2$,[37d] WOs_3,[53a] W_3Ru,[37e] $ReOs_3$,[53b,c] Re_2Os_3,[53d] Os_3Pt,[54] Pd_2Mn_2,[33] Pt_2Mo_2,[32] and $FeCo_2Mo$.[55] The Pd(1)–Pd(2) distance [2.586 (1) Å] is similar to those found in complexes containing a Pd–Pd bond bridged by one or two dppm ligands, e.g., $[Pd_2Br_2(dppm)_2]$ [2.699 (5) Å],[56] $[Pd_2(SnCl_3)Cl(dppm)_2]$ [2.644 (2) Å],[57] $[Pd_3(\mu_3\text{-}CO)(dppm)_3]^{2+}$ [2.576 (1)–2.610 (2) Å],[58a] $[Pd_3(\mu_3\text{-}Cl)(\mu_3\text{-}CO)(dppm)_3]^+$ [2.584 (1)–2.603 (1) Å][58b] and $[Pd_2Mn_2(CO)_9(dppm)_2]$ [2.681 (1) Å].[33] As the carbonyls C(51)O(1) and C(53)O(3) bridge both the Pd(1)Co(1) and Pd(2)Co(1) bonds, the shortening of the latter could be due to the small bite of dppm and/or to the difference in the trans influence of C(52)O(2) and P(4). The exocyclic Pd(1)–Co(2) bond is the longest, consistent with the above-mentioned weakness of this metal–metal bond and is significantly longer than those previously reported for Pd–Co compounds [2.595 (1)–2.604 (1) Å].[59,60] The $Co(CO)_4$ group is coordinated to Pd(1) in such a way that the vectors Pd(2)–Pd(1) and Pd(1)–Co(2) form an angle of 161.23 (5)°. This deviation from linearity is probably due to the steric crowding of the phenyl groups on P(1). The coordination about the Co(2) atom is of a distorted trigonal-bipyramidal type, but the geometry of the $Co(CO)_4$ fragment is best viewed as distorted tetrahedral, reminiscent of that of the $[Co(CO)_4]^-$ anion, as seen in the complexes $\{[o\text{-}\overline{C_6H_4C(CH_3)\underline{N(NHPh)]Pd}}Co(CO)_4\text{-}(py)\}$[59] or $[RhCo(CO)_5(PEt_3)_2]$.[61] Carbonyl bond angles around Co(2) show only small deviations from tetrahedral values with the exception of the C(55)–Co(2)–C(59) angle of 130.8 (4) Å. The carbonyl ligands C(55)O(5) and C(59)O(9) are directed toward the Pd(1) atom with Pd(1)–C(55) and Pd(1)–C(59) distances of 2.53 (1) and 2.60 (1) Å, respectively. The corresponding Co(2)–C(55)–O(5) and Co(2)–C(59)–O(9) angles are slightly bent. These values suggest a weak interaction of these two carbonyl groups with the Pd(1) center, being a consequence of the tetrahedral structure about Co(2). The other two carbonyl

---

(50) Albano, V. G.; Ciani, G.; Freni, M.; Romiti, P. *J. Organomet. Chem.* **1975**, *96*, 259.

(51) (a) Ditzel, E. J.; Johnson, B. F. G.; Lewis, J.; Raithby, P. R.; Taylor, M. J. *J. Chem. Soc., Dalton, Trans.* **1985**, 555. (b) Einstein, F. W. B.; Martin, L. R.; Pomeroy, R. K.; Rushman, P. *J. Chem. Soc., Chem. Commun.* **1985**, 345.

(52) Eisenstadt, A.; Frolow, F.; Efraty, A. *J. Chem. Soc., Chem. Commun.* **1982**, 642.

(53) (a) Chi, Y.; Shapley, J. R.; Churchill, M. R.; Li, Y. *Inorg. Chem.* **1986**, *25*, 4165. (b) Churchill, M. R.; Hollander, F. J.; Lashewycz, R. A.; Pearson, G. A.; Shapley, J. R. *J. Am. Chem. Soc.* **1981**, *103*, 2430. (c) Churchill, M. R.; Hollander, F. J. *Inorg. Chem.* **1981**, *20*, 4124. (d) Churchill, M. R.; Hollander, F. J. *Inorg. Chem.* **1978**, *17*, 3546.

(54) Williams, G. D.; Lieszkovszky, M.-C.; Mirkin, C. A.; Geoffroy, G. L.; Rheingold, A. L. *Organometallics* **1986**, *5*, 2228.

(55) Vahrenkamp, H.; Richter, F. *Organometallics* **1982**, *1*, 756.

(56) Holloway, R. G.; Penfold, B. R.; Colton, R.; McCormick, M. J. *J. Chem. Soc., Chem. Commun.* **1976**, 485.

(57) Olmstead, M. M.; Benner, L. S.; Hope, H.; Balch, A. L. *Inorg. Chim. Acta* **1979**, *32*, 193.

(58) (a) Manojlović-Muir, L.; Muir, K. W.; Lloyd, B. R.; Puddephatt, R. J. *J. Chem. Soc., Chem. Commun.* **1983**, 1336. (b) Manojlovic-Muir, L.; Muir, K. W.; Lloyd, B. R.; Puddephatt, R. J. *Ibid.* **1985**, 536.

(59) Le Borgne, G.; Bouaoud, S.-E.; Grandjean, D.; Braunstein, P.; Dehand, J.; Pfeffer, M. *J. Organomet. Chem.* **1977**, *136*, 375.

(60) Pfeffer, M.; Fischer, J.; Mitschler, A.; Ricard, L. *J. Am. Chem. Soc.* **1980**, *102*, 6338.

(61) See for example: (a) Roberts, D. A.; Mercer, W. C.; Zahurak, S. M.; Geoffroy, G. L.; DeBrosse, C. W.; Cass, M. E.; Pierpont, C. G. *J. Am. Chem. Soc.* **1982**, *104*, 910. (b) Roberts, D. A.; Mercer, W. C.; Geoffroy, G. L.; Pierpont, C. G. *Inorg. Chem.* **1986**, *25*, 1439.

groups on Co(2) show no deviation from linearity, and their average Co–C distances are normal (1.75 Å). The coordination of the Co(1) atom is conveniently described as highly distorted octahedral. The Co(1)–Pd(1) and Co(1)–Pd(2) bonds, together with Co(1)–P(4) and Co(1)–C(52), form a plane. The two carbonyl groups C(51)O(1) and C(53)O(3), lying respectively above and below this plane, complete the octahedron around the Co(1) atom. Of the three carbonyl groups borne by Co(1), C(52)O(2) is truly terminally bound. The carbonyl groups C(51)O(1) and C(53)O(3) interact with both Pd atoms, in a triply semibridging manner. However, the carbonyl and phosphine bond angles around Co(1) are very close to tetrahedral values. Thus, as described for the terminally bound $Co(CO)_4$ unit, the "$Co(CO)_3P$" fragment can again be viewed as a distorted tetrahedron, which is here doubly face capped by the Pd atoms. The planes containing respectively Co(1), C(51), and C(53) and Co(1), C(52), and P(4) are almost orthogonal (dihedral angle 91.4°). Two of the carbonyl groups are directed toward palladium atoms, as seen for C(55)O(5) and C(59)O(9).

Cluster **7** crystallizes with an acetone molecule. The structural parameters for the octahedral hexafluorophosphate anion are entirely normal. This anion appears well separated from the cationic cluster, with no significant intermolecular contact with it. The structure of the cation $[Pd_2Co(CO)_4(dppm)_2]^+$ (Figure 2) may be compared to that of **1** and considered as derived from it by the replacement of the terminally bound $Co(CO)_4$ unit by a carbonyl group. The basic Pd(1)Pd(2)Co(1) triangle with two dppm ligands bridging the Pd(1)–Pd(2) and Pd(2)–Co(1) bonds is retained. A metal triangle with two edges bridged by dppm ligands has been previously characterized by X-ray diffraction only in homonuclear clusters, such as $[Ru_3(CO)_8(dppm)_2]$.[62] As in **1** the metal atoms and the four phosphorus atoms are almost coplanar, and the maximum deviation from their best mean plane is only 0.199 (3) Å for P(2) (Table S-V[83]). The phosphorus atoms alternately lie slightly above and below this plane, as found in **1**. The values of the metal–metal bond distances in the triangular core of **7** appear to be very close to those found in **1**. The Pd(1)–Pd(2) bond is slightly shorter whereas the Pd(2)–Co(1) bond is significantly (3σ criterion) longer (0.04 Å) than in **1**. This suggests that the replacement of a $Co(CO)_4$ group with a CO ligand (although affording a cationic species) has little effect on the bonding within the Pd_2Co unit. The carbonyl group C(54)-O(4) lies in the plane defined by the three metal atoms. The linearity of the vector Pd(1)–C(54)–O(4) (angle of 177 (2)°) indicates that the carbonyl group is terminally bound to Pd(1) and is not interacting with the other metal atoms, and this vector almost bisects the angle P(1)–Pd(1)–Co. This situation is exceptional for palladium clusters as bridging carbonyls are invariably encountered.[29] As in **1**, of the three carbonyl groups borne by the Co atom, only C(52)O(2) is in the metallic plane and is terminally bound. The two other carbonyls, C(51)O(1) and C(53)O(3), are bent toward the palladium atoms, above and below the trimetallic plane, respectively, in a triply semibridging manner. They are slightly closer to the palladium atoms than in **1** (see Table I).

The carbon atoms of the methylene groups C(13) and C(38) lie respectively above and below the metallic plane (e.g., −0.66 (1) and +0.57 (1) Å for **7** (Table S-V[83])). The P–C–P angles of the dppm ligands are close to those commonly found for binuclear compounds bridged by dppm, indicating no particular constraint on the ligand.[3b] The value of the angle P(3)–Pd(2)–P(2) (106.0 (1)° in **1** and 103.8 (1)° in **7**) is close to that of the angle P(1)–Pd(1)–X, where X = Co(2) (104.4 (1)° in **1**) or C(54) (106.7 (5)° in **7**). The phosphorus–metal distances are normal and comparable to those found for tertiary phosphines bonded to transition metals. The P(4)–Co(1) distances are shorter than the average P–Pd bonds. The geometry of the phenyl groups is unexceptional and they are arranged in such a way that their relative orientations minimize repulsive steric interactions.

Infrared Spectroscopy. The IR spectra of the trinuclear clusters **3–6** exhibit two main carbonyl absorptions, and the most intense one is located around 1995 cm^{-1} and is assigned to the terminally bound CO. The absorptions around 1900 (sh) and 1870 cm^{-1} are assigned to the triply semibridging CO ligands. Changing the halide or SCN ligand does not significantly affect the spectrum, indicating little change in the electron density on the cluster and/or very efficient electronic delocalization. In the cationic clusters **7** and **8**, the ν(CO) values are shifted to higher wavenumbers owing to the decreased electron density on the clusters. The additional strong absorption band in **7** at ca. 2070 cm^{-1} is assigned to the Pd-bound linear CO. As expected, the tetranuclear cluster **1** exhibits a more complex ν(CO) pattern. By comparison with the trinuclear clusters, its highest ν(CO) absorption band, at 2009 cm^{-1}, is attributed to the $Co(CO)_4$ fragment (Figure 4[83]).

Discussion

Reactions of mononuclear Pd(II) or Pt(II) dihalogeno complexes of the type *cis*- or *trans*-$[MCl_2L_2]$ with carbonylmetalates have previously been shown to give rise to a number of homo- and heteronuclear clusters of various geometries. When the ligands L are monodentate (PR_3) or bidentate phosphines (e.g., $Ph_2PCH_2CH_2PPh_2$), redox reactions generally occur, accompanied by ligand transfer and cluster formation. The structures of the tri-, tetra-, or pentanuclear clusters thus obtained critically depend on the nature of the metals and the ligands.[32,63–66] In contrast, reactions of carbonylmetalates with dihalogeno dinuclear metal–metal-bonded palladium or platinum complexes had not been investigated so far. Since our preliminary results,[32,33] three more examples of reactions involving Pd(I) or Pt(I) dinuclear complexes have been reported[40,67,68] (e.g., eq 5[68]). These reactions afforded

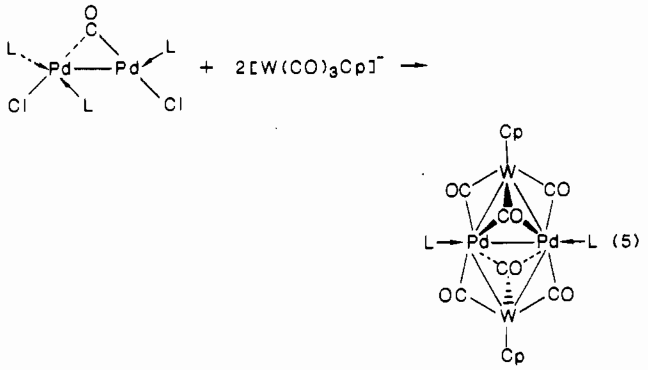

(5)

mixed-metal clusters and were *not* accompanied by a redox process, consistent with the metals of the precursor complexes and of the product being in the +1 oxidation state.

The reaction of eq 1 affords tetranuclear clusters in which the Pd–Pd bond of the precursor is retained. Both dppm ligands are still present in the product molecule, one dppm is now bridging a Pd–Co bond, as a result from phosphorus migration from palladium to cobalt,[33b] while the other still spans the Pd–Pd bond. Clearly, dppm helps to assemble the metallic core and confers to the clusters a much higher stability than that usually found for molecules containing unsupported Pd–Co bonds.[59,69] Notably, further formal insertion of a second $Co(CO)_3$ fragment into an-

---

(62) Lavigne, G.; Lugan, N.; Bonnet, J. J. *Acta Crystallogr., Sect. B: Struct. Crystallogr. Cryst. Chem.* **1982**, *B38*, 1911.

(63) Barbier, J.-P.; Bender, R.; Braunstein, P.; Fischer, J.; Ricard, L. *J. Chem. Res., Synop.* **1978**, 230; *J. Chem. Res., Miniprint* **1978**, 2913.

(64) Barbier, J.-P.; Braunstein, P. *J. Chem. Res., Synop.* **1978**, 412; *J. Chem. Res., Miniprint* **1978**, 5029.

(65) Bender, R.; Braunstein, P.; Jud, J.-M.; Dusausoy, Y. *Inorg. Chem.* **1983**, *22*, 3394.

(66) Bender, R.; Braunstein, P.; Jud, J.-M.; Dusausoy, Y. *Inorg. Chem.* **1984**, *23*, 4489.

(67) (a) Thometzek, P.; Werner, H. *J. Organomet. Chem.* **1983**, *252*, C29. (b) Thometzek, P.; Werner, H. *Organometallics* **1987**, *6*, 1169. (c) Werner, H.; Thometzek, P.; Krüger, C.; Kraus, H.-J. *Chem. Ber.* **1986**, *119*, 2777.

(68) Bender, R.; Braunstein, P.; Tiripicchio, A.; Tiripicchio Camellini, M. *J. Chem. Soc., Chem. Commun.* **1984**, 42.

(69) (a) Braunstein, P.; Dehand, J. *C. R. Seances Acad. Sci., Ser. C* **1972**, *274*, 175. (b) Braunstein, P.; Dehand, J. *Bull. Soc. Chim. Fr.* **1975**, 1997.

other Pd–P bond does not occur. Possible intermediates for the formation of **1** are discussed in the following paper.[49] The complex $[Pd_2Cl_2(\mu\text{-}CO)(dppm)_2]$, isolated from reaction 1, was ruled out as an intermediate in the synthesis of **1**, on the basis of its lower reactivity: in the A-frame complexes $[Pd_2Cl_2(\mu\text{-}Y)(dppm)_2]$ (Y = CO, CH_2), the substitution of the chlorides by $[Co(CO)_4]^-$ is more difficult than in $[Pd_2Cl_2(dppm)_2]$. Reactions are very slow but eventually lead to **1**. In the case of the CO-labile complex $[Pd_2Cl_2(\mu\text{-}CO)(dppm)_2]$, it is not clear whether **1** results from the reaction of $[Co(CO)_4]^-$ with the decarbonylated product or if attack of $[Co(CO)_4]^-$ on $[Pd_2Cl_2(\mu\text{-}CO)(dppm)_2]$ promotes this decarbonylation. However, performing the reaction under a CO atmosphere does not change significantly the yield of **1**. The lower reactivity of the A-frame complexes $[Pd_2Cl_2(\mu\text{-}Y)(dppm)_2]$ (Y = CO, CH_2) toward $Na[Co(CO)_4]$ is in keeping with a strengthening of their Pd–Cl bonds, resulting from the π-accepting properties of the apex bridge, and is consistent with the high trans effect that metal–metal bonds have on σ-donor ligands.

The substitution of the $Co(CO)_4$ fragment in **1** by anionic nucleophiles X^- (e.g., I^-, Cl^-) has been carried out according to the equilibrium of eq 2. The position of this equilibrium was found to depend strongly upon the nature of the solvent and of the cation $[C]^+$. This substitution is rapid in nondonor solvents (e.g., CH_2Cl_2), ruling out a dissociative mechanism whereby the $[Co(CO)_4]^-$ anion would be released prior to the nucleophilic attack of X^- on the metal center. Kinetic differences in terms of ΔG^* observed in the reactivity of I^- and Cl^- are well explained by the lower nucleophilicity of the latter towards the soft Pd center. As expected, F^- cannot displace I^- in **5**, in contrast to the softer SCN^- ligand. The rate of reaction of **1** with Cl^- dramatically increases when PPN^+ is used instead of a mineral cation (e.g., Na^+, K^+). In THF solution, Cl^- presents an enhanced nucleophilicity owing to the complete dissociation of [PPN][Cl]. This is not the case for the tightly-bound and almost insoluble ion pairs KCl or NaCl. Moreover, it is anticipated that the nucleophilicity of $[Co(CO)_4]^-$ in $[PPN][Co(CO)_4]$ is lower than in $Na[Co(CO)_4]$.[70] Thus the reverse reaction of eq 2 should be kinetically disfavored in this case.

The halide abstraction reaction of eq 3 is quantitative, and the carbonylated cluster **7** presents the unique feature of having a Pd-bound terminal CO ligand. This ligand is weakly bound and is easily removed and replaced by a solvent molecule when a solution of **7** is evaporated under vacuum. CO purge will restore **7**, and reversible CO uptake experiments could be performed for many cycles without product decomposition occurring.

Bonding Description. In the 44-electron trinuclear clusters described in this work, the presence of one 18-electron metal (Co) and two 16-electron metals (Pd) accounts for three metal–metal bonds, although a localized electron count about each metal raises some difficulties with respect to the EAN rule. On the other hand, the tetranuclear cluster **1** can be described in two different but formally equivalent ways: (i) the neutral $Co(CO)_4$ fragment could be considered as part of the metallic core, making **1** a 60-electron cluster with four metal–metal bonds; (ii) the anionic $[Co(CO)_4]^-$ group could be viewed as a pseudohalide. Then **1** could be described as a 44-electron cluster with a metalate substituent. This description accounts for the polarity of the Pd(1)–Co(2) bond, which is structurally and chemically best described as a Pd(I)–Co(–I) bond.

A remarkable structural feature of these clusters is the bonding mode of the bridging $\mu\text{-}Co(CO)_3(PPh_2R)$ (R = $CH_2^{\bullet}$) fragment. It can be described in two formally equivalent ways: (i) the anionic 18-electron $[\mu\text{-}Co(CO)_3(PPh_2R)]^-$ group acting as a four-electron donor toward the cationic 26-electron $[Pd_2(dppm)(PPh_2^{\bullet})X]^+$ (X = Cl, Br, I, $Co(CO)_4$) unit containing Pd(I) centers. This is supported by the synthetic origin of these molecules and by the relatively short Pd–Pd distances in **1** and **7** (Table I); (ii) the neutral 17-electron $\mu\text{-}Co(CO)_3(PPh_2R)$ group acting as a three-electron donor toward the neutral, 27-electron Pd(I)–Pd(0) mixed-valence $Pd_2(dppm)(PPh_2^{\bullet})X$ unit.

Chart I

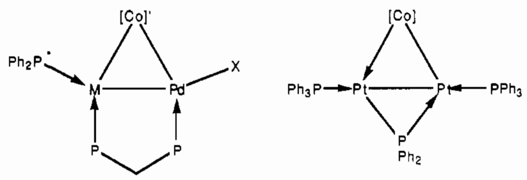

$[Co]' = Co(CO)_3(PPh_2CH_2^{\bullet})$

$[Co] = Co(CO)_3(PPh_3)$ in $[Pt_2Co(\mu\text{-}PPh_2)(CO)_3(PPh_3)_3]$

The situation in **1** and **7** constitutes a striking analogy with that in $[Pt_2Co(\mu\text{-}PPh_2)(CO)_3(PPh_3)_3]$ where a $\mu\text{-}Co(CO)_3(PPh_3)$ group, behaving as a phosphido ligand $\mu\text{-}PPh_2$, bridges a $Pt_2(\mu\text{-}PPh_2)(PPh_3)_2$ fragment (Chart I).[71] This latter is isoelectronic and isolobal with the $Pd_2(dppm)(PPh_2^{\bullet})X$ dinuclear group in the dppm clusters reported here. The present molecules constitute further examples where an anionic 18-electron (or a neutral 17-electron) metal carbonyl fragment is involved in a closo structure.[65–67,71,72]

Experimental Section

A. Reagents and General Techniques. All reactions were performed in Schlenk-type flasks under nitrogen. Solvents were dried and distilled under nitrogen: tetrahydrofuran and diethyl ether over sodium benzophenone ketyl; *n*-hexane, pentane, benzene, and toluene over sodium; dichloromethane and acetonitrile over P_2O_5; and acetone over $CaCl_2$. Water was degassed under reflux and saturated with nitrogen. Dimethyl sulfoxide was dried and degassed prior to use. Nitrogen (Air Liquide R-grade) was passed through BASF R3-11 catalyst and molecular sieve columns to remove residual oxygen and water. CO was purchased from Air Liquide (N 20) and used without further puficiation. Unless otherwise stated, reagents were obtained from commercial sources and used as received. $[Co_2(CO)_8]$ (Ventron) was purified by extraction with *n*-hexane prior to use. Diazomethane was prepared from *N*-methyl-*N*-nitroso-*p*-toluenesulfonamide and potassium hydroxide in diethylene glycol monoethyl ether and was distilled and trapped in diethyl ether at 0 °C.[73] Celite (545, Prolabo) was degassed and stored under nitrogen. Elemental analyses were performed by the Service Central de Microanalyses du CNRS. Infrared spectra were recorded in the region 4000–400 cm^{-1} on a Perkin-Elmer 398 spectrophotometer. The ^1H, $^{13}C\{^1H\}$, and $^{31}P\{^1H\}$ NMR spectra were recorded at 200.13, 50.32, and 81.02 MHz, respectively, on a FT-Bruker WP 200 SY instrument. Proton and carbon chemical shifts are positive downfield relative to external Me_4Si. ^{31}P NMR spectra were externally referenced to 85% H_3PO_4 in H_2O, with downfield chemical shifts reported as positive. All NMR solvents were freeze–pump–thaw degassed before spectra were recorded.

B. Syntheses. The ligand $Ph_2PCH_2PPh_2$(dppm)[74] and the complexes $[Pd_2Cl_2(dppm)_2]$[48] and $[Pd_2Cl_2(\mu\text{-}CO)(dppm)_2]$[48] were prepared according to literature methods. Solutions of $Na[Co(CO)_4]$ were prepared by Na/Hg reduction of THF solutions of $[Co_2(CO)_8]$.[75]

Improved Synthesis of $[Pd_2Cl_2(\mu\text{-}CH_2)(dppm)_2]$.[76] A solution of diazomethane (ca. 0.5 M in Et_2O, 3 mL) was slowly added to a cooled (0 °C) and stirred solution of $[Pd_2Cl_2(dppm)_2]$ (0.450 g, 0.428 mmol) in CH_2Cl_2 (30 mL). The color of the mixture turned from orange to pale yellow, and a yellow powder precipitated, which was recovered by filtration. The solid was purified by dissolution in hot CH_2Cl_2 (125 mL) and filtration to remove traces of an insoluble white material (probably polymethylene). Cooling the solution at −20 °C afforded air-stable yellow needles of solvated $[Pd_2Cl_2(\mu\text{-}CH_2)(dppm)_2]\cdot 0.25CH_2Cl_2$ (0.365 g, 78% based on Pd). Anal. Calcd for $C_{51.25}H_{46.5}Cl_{2.5}P_4Pd_2$ (M_r = 1087.80): C, 56.59; H, 4.31. Found: C, 56.58; H, 4.55. ^1H NMR: in

---

(70) For a related situation with $[C]^+[Fe(CO)_3NO]^-$, see: Pannell, K. H.; Chen, Y.-S.; Belknap, K.; Wu, C. C.; Bernal, I.; Creswick, M. W.; Huang, H. N. *Inorg. Chem.* **1983**, *22*, 418.

(71) Bender, R.; Braunstein, P.; Metz, B.; Lemoine, P. *Organometallics* **1984**, *3*, 381.

(72) Hofmann, P.; Schmidt, H. R. *Angew. Chem., Int. Ed. Engl.* **1986**, *25*, 837.

(73) De Boer, T. J.; Backer, H. J. *Organic Syntheses*; Wiley: New York, **1963**; Collect. Vol. II, p 250.

(74) Sommer, K. *Z. Anorg. Allg. Chem.* **1970**, *376*, 37.

(75) Pearson, R. G.; Dehand, J. *J. Organomet. Chem.* **1968**, *16*, 485.

(76) A similar procedure has been described for the synthesis of $[Pt_2Cl_2(\mu\text{-}CH_2)(dppm)_2]$: Brown, M. P.; Fisher, J. R.; Puddephatt, R. J.; Seddon, K. R. *Inorg. Chem.* **1979**, *18*, 2808.

agreement with literature data.[77] $^{31}P\{^1H\}$ NMR ($CH_2Cl_2/CDCl_3$): δ 15.43 (s).

[$Pd_2Co_2(CO)_7(dppm)_2$] (1). A filtered solution of Na[$Co(CO)_4$] in THF (0.182 M, 55 mL) was added to a cooled (−78 °C) and stirred suspension of [$Pd_2Cl_2(dppm)_2$] (5.270 g, 5.0 mmol) in THF (75 mL). The reaction temperature was progressively raised to 0 °C (3 h) by replacing the acetone–dry ice bath with ice. The color of the mixture slowly turned from orange to deep violet. The temperature was then raised to 20 °C (5 h), and the color of the reaction mixture changed to deep green. The mixture was filtered on a class 4 glass frit to remove insoluble NaCl and [$Pd_2Cl_2(\mu$-CO)(dppm)$_2$] (0.561 g, 10.4% based on Pd, identified by comparison with an authentic sample). IR (KBr): ν(CO) 1705 (br) cm^{-1} [lit.[48] (Nujol) 1705 cm^{-1}]. $^{31}P\{^1H\}$ NMR ($CH_2Cl_2/CDCl_3$): δ 18.8 ppm). Addition of *n*-hexane gave, after cooling at −20 °C, a black-green air-sensitive crystalline powder of **1**, which was washed with water to remove residual ionic species, dried in vacuo, and recrystallized from CH_2Cl_2/*n*-hexane (5.767 g, 89% based on Pd) (mp 174 °C dec). Anal. Calcd for $C_{57}H_{44}Co_2O_7P_4Pd_2$ (M_r = 1295.58): C, 52.84; H, 3.42; Co, 9.10; P, 9.56; Pd, 16.43. Found: C, 52.77; H, 3.51; Co, 8.98; P, 9.50; Pd, 16.14. IR (KBr): ν(CO) 2009 (vs), 1985 (s), 1924 (vs), 1896 (vs), 1879 (vs) cm^{-1}. ^1H NMR ($CDCl_3$): δ 7.54–6.85 (40 H, m, C_6H_5), 4.51 (2 H, dt, ^2J(PH) = 9.3 Hz, ^4J(PH) = 3.3 Hz, CH_2), 3.97 (2 H, t, ^2J(PH) = 9.6 Hz, CH_2). $^{31}P\{^1H\}$ NMR ($CH_2Cl_2/CDCl_3$): δ 28.0 (1 P, br m, P → Co), −0.93 (1 P, m, P→Pd), −3.16 (1 P, m, P→Pd), −10.90 (1 P, m, P→Pd). $^{13}C\{^1H\}$ NMR (CD_2Cl_2): δ 212.0 (s, CO), 210.7 (s, CO), 204.4 (s, CO), 135.6–128.0 (m, C_6H_5), 48.8 (t, ^1J(PC) = 17.8 Hz, CH_2). The other CH_2 resonance at ca. 54 ppm is masked by the solvent.

Heating of 1 in Toluene. A solution of **1** (0.047 g, 0.036 mmol) in toluene (20 mL) was heated to 60–80 °C and stirred for 24 h. The solution slowly turned from green to brown. The reaction mixture was filtered to remove insoluble brown material and evaporated to dryness, affording the red-brown solid **2** (0.037 g, 91% based on Co), which was recrystallized from toluene/*n*-hexane. Anal. Calcd for $C_{55}H_{44}Co_2O_5P_4Pd$ (M_r = 1133.14): C, 58.30; H, 3.91. Found: C, 53.32; H, 4.31. IR (KBr): ν(CO) 1985 (vs), 1933 (vs), 1895 (m), 1709 (m) cm^{-1}. ^1H NMR ($CDCl_3$): δ 7.95–6.90 (40 H, m, C_6H_5), 4.28 (4 H, br m, CH_2). $^{31}P\{^1H\}$ NMR ($CH_2Cl_2/CDCl_3$): δ 28.3 (1 P, br m), −13.3 (1 P, d, J(PP) = 31.5 Hz). Decomposition occurred on MS runs.

Reaction of [$Pd_2Cl_2(\mu$-CO)(dppm)$_2$] with Na[$Co(CO)_4$]. A filtered solution of Na[$Co(CO)_4$] in THF (0.16 M, 2.3 mL) was added to a cooled (−78 °C) suspension of [$Pd_2Cl_2(\mu$-CO)(dppm)$_2$] (0.200 g, 0.185 mmol) in THF (20 mL). The temperature was raised to 0 °C. No change in color was observed. The temperature was then raised to 20 °C and the solution slowly turned from orange to green after 7 h. The stirring was maintained for 4 days, and subsequent workup of the green solution was performed by following the procedure described for the synthesis of **1**. It afforded unreacted [$Pd_2Cl_2(\mu$-CO)(dppm)$_2$] (0.057 g, 29% based on Pd) and **1** (0.158 g, 66% based on Pd). The same reaction was carried out under a CO atmosphere to prevent decarbonylation of [$Pd_2Cl_2(\mu$-CO)(dppm)$_2$]. After 4 days of stirring at room temperature, the yield of **1** was 58%, with 34% of [$Pd_2Cl_2(\mu$-CO)(dppm)$_2$] being recovered.

Reaction of [$Pd_2Cl_2(\mu$-CH_2)(dppm)$_2$] with Na[$Co(CO)_4$]. a. Reaction in THF. A filtered solution of Na[$Co(CO)_4$] in THF (0.05 M, 15.2 mL) was added to a suspension of [$Pd_2Cl_2(\mu$-CH_2)(dppm)$_2$] (0.406 g, 0.381 mmol) in THF (30 mL). After 24 h of stirring, no reaction had occurred. The solution was then refluxed for 4 h. The resulting brown solution was filtered to remove NaCl (0.115 g) and other insoluble material. An IR spectrum of the solution showed the presence of [$Co(CO)_4$]$^-$. The mixture was evaporated to dryness, and the residue was extracted with toluene and filtered. Addition of *n*-hexane induced the precipitation of a brown powder (0.275 g) whose IR spectrum (KBr) exhibited absorption bands at 1980 (vs), 1924 (vs), and 1880 (vs) cm^{-1}. The $^{31}P\{^1H\}$ NMR spectrum showed a complex mixture of products with traces of **1** and of **2** (see above) and signals in the range of 42.5–38.8 and 25.4–19.1 ppm. Further attempts to separate and isolate pure products failed.

b. Reaction in Et_2O. Solid Na[$Co(CO)_4$] (0.009 g, 0.047 mmol) was added to a suspension of [$Pd_2Cl_2(\mu$-CH_2)(dppm)$_2$] (0.025 g, 0.023 mmol) in Et_2O (20 mL). Stirring was maintained for 20 h, producing a slight change in the color of the solution from pale yellow to light green. The mixture was evaporated to dryness, and the residue was extracted with toluene and filtered and the solvent evaporated in vacuo. The IR spectrum of the resulting green solid showed only bands due to **1** (<0.005 g, ca. 10% based on Pd).

Table II. Crystal Data and Intensity Collection Parameters for [$Pd_2Co_2(CO)_7(dppm)_2$]·2.5C_4H_8O and [$Pd_2Co(CO)_4(dppm)_2$][PF_6]·C_3H_6O

	1·2.5THF	**7**·Me_2CO
formula	$C_{67}H_{64}Co_2O_{9.5}P_4Pd_2$	$C_{57}H_{50}CoF_6O_5P_5Pd_2$
fw	1475.81	1355.62
cryst syst	triclinic	monoclinic
space group	$P\bar{1}$	Cc
cryst dimens, mm	spherical, mean diameter 0.23	0.15 × 0.10 × 0.10
cryst color and habit	green prism	red parallelepiped
a, Å	18.417 (8)	22.87 (2)
b, Å	14.798 (6)	14.198 (4)
c, Å	13.855 (6)	22.27 (2)
α, deg	113.61 (2)	
β, deg	107.50 (2)	122.35 (5)
γ, deg	82.20 (2)	
Z	2	4
V, Å^3	3299	6109
F(000), e	748	2720
ρ(calcd), g cm^{-3}	1.485	1.411
temp, °C	25	25
diffractometer	Philips PW 1100/16	Enraf-Nonius CAD-4
radiation (graphite monochromator)	CuKα_1 (λ = 1.5405 Å)	MoKα (λ = 0.71073 Å)
linear abs coeff, cm^{-1}	98.84	10.27
transmissn factors: max, min	0.27, 0.21	
scan mode	θ–2θ; flying step–scan	θ–2θ
step width, deg	0.4	
scan width, deg	0.90 + 0.14 tan θ	1 + 0.35 tan θ
scan speed, deg/s	0.024	
θ limits, deg	5–57	1–25
octants collcd	$h,k,\pm l$	$\pm h,k,l$
no. of data collcd	8688	5723
no. of unique data used	6083 ($I > 3\sigma(I)$)	3996 ($I > 3\sigma(I)$)
$R = \sum\lVert F_o\rvert - \lvert F_c\rVert/\sum\lvert F_o\rvert$	0.055	0.053
$R_w = (\sum w(\lvert F_o\rvert - \lvert F_c\rvert)^2/\sum w\lvert F_o\rvert^2)^{1/2}$	0.076	0.069
std error in an observn of unit wt, e	1.64	1.60
p factor	0.08	0.07
largest shift/esd, final cycle	0.054	1.940
largest peak in final diff map, e/Å^3	0.11	0.68

[$Pd_2CoCl(CO)_3(dppm)_2$] (3). A solution of NaCl (0.08 g, 10-fold excess) in a mixture of acetone (25 mL) and water (10 mL) was added to a solution of **1** (0.175 g, 0.135 mmol) in acetone (150 mL). While being stirred, the reaction mixture slowly turned from deep green to brown (1 day). *n*-Hexane was then added, and vigorous stirring led **3** to precipitate in the organic phase. It was collected by filtration and dried in vacuo. Dissolution in toluene and filtration afforded a red-brown solution, which after addition of *n*-hexane gave a pure, air-sensitive brown powder of **3** (0.125 g, 80% based on Pd) (mp 195 °C dec). Anal. Calcd for $C_{53}H_{44}ClCoO_3P_4Pd_2$ (M_r = 1160.05): C, 54.88; H, 3.82. Found: C, 55.17; H, 3.86. IR (KBr): ν(CO) 1992 (s), 1900 (sh), 1854 (m, br) cm^{-1}. ^1H NMR ($CDCl_3$): δ 7.79–6.86 (40 H, m, C_6H_5), 4.30 (2 H, dt, ^2J(PH) = 9.1 Hz, ^4J(PH) = 2.5 Hz, CH_2), 3.98 (2 H, t, ^2J(PH) = 9.7 Hz, CH_2). $^{31}P\{^1H\}$ NMR ($CH_2Cl_2/CDCl_3$): δ 27.8 (1 P, br m, P→Co), −5.91 (1 P, m, P→Pd), −8.73 (1 P, m, P→Pd), −21.09 (1 P, m, P→Pd). If this reaction, starting from NaCl (KCl or NEt_4Cl) and **1**, is carried out in too small a volume of water, evaporation to dryness of the brown mixture or addition of a nonsolvent such as *n*-hexane causes a reversal of the reaction toward the green starting material **1**. Therefore, a certain quantity of water (ca. 5–10% of the acetone's volume) is needed to drive the reaction by maintaining [$Co(CO)_4$]$^-$ in solution after hexane addition and precipitation of **3**.

Reaction of 1 with [PPN]Cl. [PPN]Cl (PPN = $(Ph_3P)_2N$) (0.262 g, 0.456 mmol) was added to a solution of **1** (0.600 g, 0.463 mmol) in THF (50 mL). The reaction mixture turned from deep green to brown in 0.5 h. An IR spectrum of the solution showed the presence of both [$Co(CO)_4$]$^-$ and **3**. Evaporation of this solution to dryness, followed by successive extraction of the residue with the solvents toluene, THF, and CH_2Cl_2 and crystallization of each fraction by addition of pentane, always gave **3** contaminated with variable amounts of [PPN][$Co(CO)_4$].

[$Pd_2CoBr(CO)_3(dppm)_2$] (4). A solution of KBr (0.10 g, 10-fold excess) in a mixture of acetone (10 mL) and H_2O (2 mL) was added to a solution of **1** (0.110 g, 0.085 mmol) in acetone. The reaction mixture immediately turned red-brown. After 1 h, *n*-hexane was added and the resulting precipitate was filtered off and dried. Purification was achieved by dissolving this solid in toluene and filtering the solution. Addition of

---

[77] Balch, A. L.; Hunt, C. T.; Lee, C.-L.; Olmstead, M. M.; Farr, J. P. *J. Am. Chem. Soc.* **1981**, *103*, 3764.

Table III. Positional Parameters and Their Estimated Standard Deviations for $\mathbf{1}\cdot 2.5C_4H_8O$[a]

atom	x	y	z	B,[b] Å^2
Pd(1)	0.26904 (3)	0.51112 (4)	0.23687 (5)	4.60 (2)
Pd(2)	0.27397 (3)	0.32053 (4)	0.16436 (4)	3.88 (1)
Co(1)	0.23800 (7)	0.41372 (9)	0.3402 (1)	4.35 (3)
Co(2)	0.2767 (1)	0.7041 (1)	0.3766 (1)	7.16 (5)
P(1)	0.2944 (1)	0.5126 (1)	0.0870 (2)	4.40 (5)
P(2)	0.2898 (1)	0.2925 (1)	−0.0020 (2)	4.21 (5)
P(3)	0.2779 (1)	0.1682 (1)	0.1730 (2)	4.11 (5)
P(4)	0.2077 (1)	0.2836 (2)	0.3584 (2)	4.47 (5)
C(1)	0.3576 (5)	0.6069 (6)	0.1069 (7)	5.4 (2)
C(2)	0.3302 (6)	0.7006 (7)	0.1239 (9)	7.4 (3)
C(3)	0.3736 (8)	0.7770 (7)	0.148 (1)	9.6 (4)
C(4)	0.4496 (7)	0.7574 (8)	0.1482 (9)	9.4 (4)
C(5)	0.4788 (6)	0.6646 (9)	0.1325 (9)	9.1 (4)
C(6)	0.4343 (6)	0.5876 (7)	0.1102 (8)	6.9 (3)
C(7)	0.2114 (5)	0.5313 (5)	−0.0136 (6)	5.0 (2)
C(8)	0.1403 (5)	0.5258 (7)	−0.0087 (8)	6.3 (3)
C(9)	0.0768 (6)	0.5402 (8)	−0.0807 (9)	8.9 (4)
C(10)	0.0835 (6)	0.5537 (8)	−0.171 (1)	9.3 (4)
C(11)	0.1556 (7)	0.5601 (8)	−0.1820 (9)	8.4 (4)
C(12)	0.2203 (5)	0.5460 (7)	−0.1023 (8)	6.4 (3)
C(13)	0.3385 (4)	0.3967 (6)	0.0088 (7)	4.8 (2)
C(14)	0.2026 (5)	0.2809 (6)	−0.1097 (6)	4.8 (2)
C(15)	0.1346 (5)	0.2757 (7)	−0.0922 (7)	6.3 (3)
C(16)	0.0670 (6)	0.2691 (9)	−0.171 (1)	8.9 (4)
C(17)	0.0704 (7)	0.2684 (9)	−0.270 (1)	9.8 (4)
C(18)	0.1369 (7)	0.2711 (8)	−0.2925 (9)	8.5 (4)
C(19)	0.2029 (5)	0.2790 (7)	−0.2114 (8)	6.2 (3)
C(20)	0.3481 (5)	0.1847 (5)	−0.0626 (6)	4.9 (2)
C(21)	0.4237 (5)	0.1845 (6)	−0.0014 (8)	6.2 (3)
C(22)	0.4704 (6)	0.1047 (7)	−0.0400 (9)	8.2 (3)
C(23)	0.4401 (6)	0.0264 (7)	−0.1402 (8)	8.5 (3)
C(24)	0.3697 (7)	0.0279 (7)	−0.1949 (8)	8.0 (3)
C(25)	0.3215 (6)	0.1082 (7)	−0.1587 (7)	6.5 (3)
C(26)	0.2573 (5)	0.0581 (5)	0.0486 (6)	4.5 (2)
C(27)	0.3091 (6)	−0.0172 (7)	0.0247 (8)	6.7 (3)
C(28)	0.2912 (7)	−0.0984 (8)	−0.077 (1)	8.7 (4)
C(29)	0.2219 (7)	−0.1023 (8)	−0.1487 (9)	8.4 (4)
C(30)	0.1713 (6)	−0.027 (1)	−0.124 (1)	9.1 (4)
C(31)	0.1890 (6)	0.0542 (7)	−0.0253 (8)	6.8 (3)
C(32)	0.3639 (5)	0.1373 (5)	0.2591 (6)	4.5 (2)
C(33)	0.4298 (5)	0.1892 (6)	0.2901 (7)	5.2 (2)
C(34)	0.4954 (5)	0.1705 (7)	0.3619 (9)	6.8 (3)
C(35)	0.4973 (6)	0.0964 (8)	0.3957 (8)	7.5 (3)
C(36)	0.4338 (7)	0.0407 (7)	0.3655 (8)	7.9 (3)
C(37)	0.3674 (5)	0.0622 (6)	0.2984 (7)	5.7 (3)
C(38)	0.2009 (5)	0.1706 (6)	0.2323 (7)	4.8 (2)
C(39)	0.2689 (5)	0.2429 (6)	0.4658 (6)	5.0 (2)
C(40)	0.3393 (5)	0.2829 (7)	0.5257 (7)	6.3 (3)
C(41)	0.3856 (6)	0.2477 (8)	0.6016 (8)	7.9 (3)
C(42)	0.3656 (7)	0.1726 (8)	0.6185 (8)	8.5 (3)
C(43)	0.2948 (6)	0.1316 (7)	0.5603 (8)	7.5 (3)
C(44)	0.2472 (6)	0.1653 (7)	0.4832 (7)	6.4 (3)
C(45)	0.1138 (5)	0.2922 (6)	0.3794 (6)	5.1 (2)
C(46)	0.0531 (6)	0.241 (1)	0.305 (1)	9.3 (4)
C(47)	−0.0174 (6)	0.257 (1)	0.328 (1)	14.4 (7)
C(48)	−0.0286 (6)	0.318 (1)	0.419 (1)	9.7 (4)
C(49)	0.0292 (7)	0.3707 (9)	0.4925 (9)	9.2 (4)
C(50)	0.1011 (6)	0.3580 (8)	0.4750 (8)	7.4 (3)
C(51)	0.1617 (5)	0.4128 (6)	0.2244 (8)	5.7 (3)
O(1)	0.1038 (3)	0.4096 (5)	0.1606 (5)	7.2 (2)
C(52)	0.2124 (5)	0.5078 (7)	0.4545 (7)	6.2 (3)
O(2)	0.1961 (4)	0.5660 (6)	0.5270 (6)	9.5 (2)
C(53)	0.3394 (5)	0.4247 (6)	0.3706 (7)	5.0 (2)
O(3)	0.4041 (3)	0.4316 (5)	0.4034 (5)	6.9 (2)
C(55)	0.1837 (6)	0.6596 (7)	0.296 (1)	8.2 (4)
O(5)	0.1229 (5)	0.6485 (6)	0.2581 (9)	12.5 (4)
C(56)	0.2845 (8)	0.8138 (8)	0.358 (1)	10.3 (4)
O(6)	0.2885 (6)	0.8858 (6)	0.3518 (9)	13.7 (4)
C(58)	0.2762 (8)	0.742 (1)	0.518 (1)	9.9 (5)
O(8)	0.2761 (8)	0.7696 (9)	0.6058 (8)	17.0 (5)
C(59)	0.3668 (7)	0.6478 (8)	0.3692 (9)	7.7 (3)
O(9)	0.4305 (4)	0.6250 (6)	0.3749 (7)	10.1 (3)
O(1S)	0.5282 (8)	0.382 (1)	0.169 (1)	19.0 (5)*
C(1S)	0.612 (1)	0.381 (2)	0.166 (2)	17.4 (7)*
C(2S)	0.653 (2)	0.408 (2)	0.261 (2)	23 (1)*
O(3S)	0.592 (1)	0.430 (2)	0.335 (2)	21.0 (9)*
C(4S)	0.528 (1)	0.412 (2)	0.276 (2)	18.5 (8)*
O(2S)	−0.005 (1)	0.124 (1)	0.968 (1)	22.0 (6)*
C(5S)	0.049 (1)	0.945 (2)	0.141 (2)	19.7 (9)*
C(6S)	0.135 (1)	0.901 (2)	0.139 (2)	21 (1)*
C(7S)	0.120 (1)	0.812 (2)	0.063 (2)	18.6 (8)*
C(8S)	0.045 (2)	0.796 (2)	−0.009 (2)	26 (1)*
C(X1)	0.000	0.000	0.500	10.0*
C(X2)	0.102	−0.021	0.479	10.0*
C(X3)	−0.137	0.020	0.416	10.0*
C(X4)	−0.068	0.104	0.479	10.0*
C(X5)	−0.018	0.020	0.416	10.0*

[a] For atoms shown in Figure 1. Positional parameters for remaining atoms in are given in the supplementary material.[83] [b] Starred values denote isotropically refined atoms. **B** values for anisotropically refined atoms are given in the form of the isotropic equivalent thermal parameters: **B** (Å^2) $= (4/3)[\beta_{11}a^2 + \beta_{22}b^2 + \beta_{33}c^2 + \beta_{12}ab(\cos\gamma) + \beta_{13}ac(\cos\beta) + \beta_{23}bc(\cos\alpha)]$.

n-hexane afforded a red-brown, air-sensitive powder of **4** (0.070 g, 68% based on Pd) (mp 203 °C). Anal. Calcd for $C_{53}H_{44}BrCoO_3P_4Pd_2$ (M_r = 1204.50): C, 52.85; H, 3.68. Found: C, 52.34; H, 3.76. IR (KBr): ν(CO) 1991 (s), 1900 (sh), 1859 (m, br) cm^{-1}. ^{1}H NMR (CDCl$_3$): δ 7.72–6.91 (40 H, m, C_6H_5), 4.37 (2 H, dt, ^2J(PH) = 9.0 Hz, ^4J(PH) = 3.0 Hz, CH$_2$), 4.03 (2 H, t, ^2J(PH) = 9.8 Hz, CH$_2$). ^{31}P{^{1}H} NMR (CH$_2$Cl$_2$/CDCl$_3$): δ 27.0 (1 P, br m, P→Co), −5.54 (1 P, m, P→Pd), −7.86 (1 P, m, P→Pd), −19.06 (1 P, m, P→Pd).

[Pd$_2$CoI(CO)$_3$(dppm)$_2$] (5). This complex was prepared by using the same procedure as for **4**, by reacting **1** (0.240 g, 0.185 mmol) with KI (0.31 g, 10-fold excess). Red-brown, air-sensitive crystals of **5** were obtained (0.220 g, 95% based on Pd) (mp 206–208 °C). Anal. Calcd for $C_{53}H_{44}CoIO_3P_4Pd_2$ (M_r = 1251.51): C, 50.87; H, 3.54. Found: C, 50.69; H, 3.93. IR (KBr): ν(CO) 1989 (s), 1900 (sh), 1868 (m, br) cm^{-1}. ^{1}H NMR (CDCl$_3$): δ 7.69–6.85 (40 H, m, C_6H_5), 4.54 (2 H, dt, ^2J(PH) = 9.0 Hz, ^4J(PH) = 3.0 Hz, CH$_2$), 4.11 (2 H, t, ^2J(PH) = 9.5 Hz, CH$_2$). ^{31}P{^{1}H} NMR (CH$_2$Cl$_2$/CDCl$_3$): δ 25.1 (1 P, br m, P→Co), −4.20 (1 P, m, P→Pd), −6.63 (1 P, m, P→Pd), −17.21 (1 P, m, P→Pd). ^{13}C{^{1}H} NMR (CDCl$_3$): δ 213.0 (s, CO), 133.7, −127.9 (m, C_6H_5), 52.8 (t, ^1J(PC) ≃ 20 Hz, CH$_2$), 51.4 (t, ^1J(PC) ≃ 20 Hz, CH$_2$).

When **1** was reacted with KI in THF or acetone to give **5**, similar observations concerning color changes and solvent dependence were made as in the reactions of **1** with chlorides (see above). Chromatographic separation of this reaction mixture, first taken to dryness and redissolved in CH$_2$Cl$_2$, could be achieved by eluting first a green solution of **1** in CH$_2$Cl$_2$, followed by THF elution of red-brown **5** (40% yield). Interestingly, **1**, which was no longer present at the end of the reaction of eq 2, re-formed during the workup procedure.

Reaction of 1 with [NEt$_4$]I. A solution of [NEt$_4$]I (0.16 g, twofold excess) in CH$_2$Cl$_2$ (20 mL) was added to a solution of **1** (0.317 g, 0.24 mmol) in CH$_2$Cl$_2$ (25 mL), causing an immediate color change of the reaction mixture from green to red-brown. Addition of *n*-hexane (30 mL) to the solution and cooling (−20 °C) gave a pale-colored precipitate of [NEt$_4$]I, which was removed by filtration. More *n*-hexane (40 mL) was then added to the solution and afforded a brown powder containing both [NEt$_4$][Co(CO)$_4$] and **5** (which was later purified by fractional crystallization in CH$_2$Cl$_2$/*n*-hexane). Further precipitation of the filtered solution afforded pure **5** (total yield 0.153 g, 51% based on Pd), and the color of the mother liquor turned back to green, indicating re-formation of **1** (characterized by IR spectroscopy).

Reaction of 1 with KOH. A solution of KOH in acetone/water (0.14 M, 2 mL) was added to a solution of **1** (0.081 g, 0.062 mmol) in acetone (10 mL). After 0.25 h of vigorous stirring, the green color of the reaction mixture had turned deep violet (note that evaporation of the solution to dryness or impregnation onto silica gel caused reversion to the initial green color). *n*-Hexane was added to the violet solution, leading to precipitation and recovery of **1**. The filtered solution remained light violet and was evaporated to dryness. The violet residue was washed with water and dried (0.018 g). Its IR spectrum showed absorption bands at 1991 (s) and 1858 (w) cm^{-1}, reminiscent of the pattern of a [Pd$_2$CoX(CO)$_3$(dppm)$_2$]-type species. Further attempts to purify this solid led to decomposition. In THF, reaction of **1** does not take place, even with a large excess of KOH.

Reaction of 1 with NaH. Solid NaH (0.013 g, 10-fold excess) was added to a solution of **1** (0.070 g, 0.054 mmol) in THF (15 mL). No immediate color change occurred. After the mixture was stirred over-

Table IV. Positional Parameters and Their Estimated Standard Deviations for $7 \cdot C_3H_6O$[a]

atom	x	y	z	B,[b] Å^2	atom	x	y	z	B,[b] Å^2
Pd(1)	0.087	0.09846 (9)	0.128	4.43 (3)	C(20)	−0.1799 (6)	0.155 (1)	−0.0615 (6)	3.4 (3)
Pd(2)	0.00000 (5)	0.14888 (6)	−0.00001 (5)	2.74 (2)	C(21)	−0.2353 (6)	0.108 (1)	−0.1221 (7)	4.4 (4)
Co	0.12885 (6)	0.1636 (1)	0.04753 (7)	1.92 (3)	C(22)	−0.2965 (8)	0.157 (1)	−0.1662 (8)	5.6 (4)
P(1)	0.0023 (2)	0.0653 (2)	0.1502 (2)	3.13 (7)	C(23)	−0.3051 (7)	0.244 (2)	−0.1537 (8)	6.5 (5)
P(2)	−0.0975 (1)	0.1000 (2)	−0.0043 (1)	2.76 (7)	C(24)	−0.2540 (9)	0.293 (1)	−0.094 (1)	7.4 (5)
P(3)	−0.0409 (1)	0.2100 (3)	−0.1090 (2)	3.01 (7)	C(25)	−0.1912 (8)	0.249 (1)	−0.0508 (8)	5.6 (5)
P(4)	0.1128 (1)	0.2206 (3)	−0.0526 (2)	3.18 (7)	C(26)	−0.0614 (6)	0.334 (1)	−0.1183 (6)	4.0 (3)
P(5)	0.4396 (3)	0.9586 (4)	0.1445 (3)	6.9 (1)	C(27)	−0.0802 (7)	0.385 (1)	−0.1799 (6)	4.6 (3)
F(1)	0.4300 (8)	0.898 (1)	0.1949 (8)	15.2 (5)	C(28)	−0.0916 (9)	0.477 (1)	−0.1853 (9)	6.7 (5)
F(2)	0.5146 (8)	0.919 (2)	0.183 (1)	15.7 (7)	C(29)	−0.0855 (9)	0.527 (1)	−0.126 (1)	7.0 (5)
F(3)	0.4473 (9)	1.029 (1)	0.0970 (7)	15.1 (6)	C(30)	−0.071 (1)	0.480 (1)	−0.0674 (9)	6.8 (5)
F(4)	0.475 (1)	1.037 (1)	0.2032 (9)	13.6 (7)	C(31)	−0.0566 (7)	0.385 (1)	−0.0625 (7)	4.4 (3)
F(5)	0.432 (2)	0.872 (1)	0.098 (1)	22 (1)	C(32)	−0.1147 (6)	0.151 (1)	−0.1831 (5)	3.7 (3)
F(6)	0.377 (1)	1.008 (2)	0.122 (1)	20.5 (8)	C(33)	−0.1785 (7)	0.191 (2)	−0.2208 (8)	6.4 (5)
O(1)	0.0928 (7)	−0.0417 (9)	0.0233 (8)	9.0 (4)	C(34)	−0.2372 (8)	0.144 (2)	−0.2775 (9)	10.7 (8)
O(2)	0.2809 (7)	0.161 (1)	0.1477 (7)	8.7 (5)	C(35)	−0.2258 (9)	0.049 (2)	−0.2913 (9)	9.5 (6)
O(3)	0.0847 (7)	0.320 (1)	0.1087 (8)	11.4 (5)	C(36)	−0.164 (1)	0.010 (2)	−0.253 (1)	9.5 (6)
O(4)	0.2239 (9)	0.068 (1)	0.2617 (9)	12.0 (6)	C(37)	−0.1079 (8)	0.062 (1)	−0.1962 (9)	6.4 (5)
O(5)	0.294 (1)	0.331 (1)	0.629 (1)	12.1 (8)	C(38)	0.0251 (5)	0.196 (1)	−0.1307 (6)	3.3 (3)
C(1)	0.0206 (7)	0.1080 (9)	0.2365 (6)	3.8 (3)	C(39)	0.1654 (7)	0.171 (1)	−0.0832 (7)	4.0 (3)
C(2)	0.0656 (7)	0.057 (1)	0.2976 (7)	4.1 (4)	C(40)	0.2175 (6)	0.108 (1)	−0.0433 (8)	5.2 (4)
C(3)	0.0810 (6)	0.085 (1)	0.3635 (6)	3.9 (3)	C(41)	0.2599 (7)	0.069 (1)	−0.064 (1)	6.1 (5)
C(4)	0.0524 (9)	0.166 (2)	0.3695 (9)	6.8 (5)	C(42)	0.2458 (7)	0.094 (1)	−0.1291 (9)	7.0 (4)
C(5)	0.0114 (8)	0.220 (1)	0.3082 (8)	5.9 (4)	C(43)	0.1966 (7)	0.154 (2)	−0.1689 (9)	6.5 (5)
C(6)	−0.0058 (8)	0.190 (1)	0.2437 (8)	5.0 (4)	C(44)	0.1562 (8)	0.193 (2)	−0.1502 (7)	6.2 (5)
C(7)	−0.0194 (6)	−0.056 (1)	0.1538 (6)	3.5 (3)	C(45)	0.1269 (5)	0.346 (1)	−0.0527 (6)	3.5 (3)
C(8)	−0.0720 (8)	−0.077 (1)	0.1670 (7)	5.0 (4)	C(46)	0.1756 (6)	0.389 (1)	0.0096 (6)	4.2 (3)
C(9)	−0.0951 (8)	−0.165 (1)	0.1655 (9)	5.6 (4)	C(47)	0.1905 (8)	0.487 (1)	0.0107 (8)	5.9 (4)
C(10)	−0.063 (1)	−0.239 (1)	0.157 (1)	6.8 (6)	C(48)	0.1581 (7)	0.535 (1)	−0.0503 (8)	5.5 (4)
C(11)	−0.0098 (9)	−0.222 (1)	0.147 (1)	7.4 (6)	C(49)	0.107 (1)	0.495 (1)	−0.113 (1)	7.6 (6)
C(12)	0.0083 (7)	−0.134 (1)	0.1436 (9)	5.2 (4)	C(50)	0.0929 (8)	0.402 (1)	−0.1137 (8)	5.1 (4)
C(13)	−0.0804 (7)	0.118 (1)	0.0846 (6)	3.9 (3)	C(51)	0.101 (1)	0.034 (3)	0.037 (2)	20 (1)
C(14)	−0.1137 (6)	−0.0251 (9)	−0.0233 (6)	3.1 (3)	C(52)	0.2212 (8)	0.162 (1)	0.1090 (8)	6.0 (5)
C(15)	−0.1600 (6)	−0.075 (1)	−0.0147 (7)	4.4 (3)	C(53)	0.092 (1)	0.245 (2)	0.098 (1)	23.0 (8)
C(16)	−0.1714 (9)	−0.169 (1)	−0.031 (1)	6.6 (5)	C(54)	0.1734 (8)	0.078 (2)	0.2155 (9)	6.7 (5)
C(17)	−0.136 (1)	−0.212 (1)	−0.055 (1)	8.6 (7)	C(56)	0.2794 (9)	0.252 (2)	0.636 (1)	8.0 (6)
C(18)	−0.0861 (9)	−0.167 (1)	−0.062 (1)	8.1 (5)	C(57)	0.310 (1)	0.213 (2)	0.709 (2)	12.2 (9)
C(19)	−0.0761 (7)	−0.073 (1)	−0.0459 (7)	4.6 (3)	C(58)	0.239 (1)	0.190 (2)	0.578 (2)	12 (1)

[a] For atoms shown in Figure 2. Positional parameters for remaining atoms are given in the supplementary material.[83] [b] B values for anisotropically refined atoms are given in the form of the isotropic equivalent thermal parameters: $B(\text{Å}^2) = (4/3)[\beta_{11}a^2 + \beta_{22}b^2 + \beta_{33}c^2 + \beta_{12}ab(\cos\gamma) + \beta_{13}ac(\cos\beta) + \beta_{23}bc(\cos\alpha)]$.

night, the color of the solution had turned to yellow-brown. An IR spectrum of this solution showed the presence of both **1** and $[Co(CO)_4]^-$. Further attempts to drive this slow reaction toward product formation by replacing THF with a more polar solvent (MeCN) were unsuccessful and led to decomposition. No ^1H NMR spectroscopic evidence for the formation of a hydride-metal bond was obtained.

Attempted Reaction of 1 with NaF. A solution of NaF (0.050 g, 10-fold excess) in acetone (20 mL) was added to a solution of **1** (0.159 g, 0.122 mmol) in acetone (50 mL) and stirred for 12 h. No change in the green color occurred, and the starting material was recovered.

Attempted Reaction of 5 with NaF. A solution of NaF (0.030 g, 10-fold excess) in acetone (10 mL) was added to a solution of **5** (0.093 g, 0.074 mmol) in acetone (25 mL). After 2 h of stirring, *n*-hexane was added to the brown solution, affording a brown powder of **5** (identified by ^1H NMR spectroscopy).

Attempted Reaction of 5 with NaCl. A solution of NaCl (0.010 g, 10-fold excess) in acetone (5 mL) was added to a solution of **5** (0.020 g, 0.016 mmol) in acetone (5 mL). After 8 h of stirring, the solvent was removed in vacuo. Extraction of the solid residue with $CDCl_3$ (^1H NMR spectroscopy) allowed the quantitative recovery of **5**.

Reactions of 1 or 5 with $NaBH_4$. Solid $NaBH_4$ (0.007 g, fivefold excess) was added to a solution of **1** (0.050 g, 0.038 mmol) in THF (20 mL). Upon stirring (0.25 h), the color of the reaction mixture changed from green to yellow-brown. The solvent was removed in vacuo, and the brown solid residue was extracted with toluene, affording unidentified product(s). A similar reaction occurred starting with **5**.

$[Pd_2Co(SCN)(CO)_3(dppm)_2]$ (6). A solution of **5** (0.060 g, 0.048 mmol) in acetone (50 mL) was treated with a large excess of KSCN (0.047 g, 0.48 mmol). Immediately, the solution turned from red-brown to dark red. After filtration, **6** was precipitated from solution with *n*-hexane, collected, and vacuum-dried (0.052 g, 92% based on Pd) (mp 210–212 °C). Recrystallization from CH_2Cl_2/*n*-hexane gave microcrystals of solvated **6**. Anal. Calcd for $6 \cdot 1.5CH_2Cl_2$ ($C_{55.5}H_{47}Cl_3CoNO_3P_4Pd_2S$) ($M_r$ = 1310.08): C, 50.88; H, 3.62; N, 1.07. Found: C, 51.21; H, 3.66; N, 0.61. IR (KBr): ν(CN) 2092 (m), ν(CO) 1991 (s), 1910 (sh), 1862 (m, br) cm^{-1}. IR (toluene): ν(CN) 2094 (m), ν(CO) 2009 (s), 1860 (m, br) cm^{-1}. ^1H NMR ($CDCl_3$): δ, 7.61–6.90 (40 H, m, C_6H_5), 4.37 (2 H, dt, ^2J(PH) = 8.8 Hz, ^4J(PH) = 2.0 Hz, CH_2), 4.04 (2 H, t, ^2J(PH) = 9.1 Hz, CH_2). $^{31}P\{^1H\}$ NMR ($CH_2Cl_2/CDCl_3$): δ 26.6 (1 P, br m, P→Co), −3.39 (1 P, m, P→Pd), −6.60 (1 P, m, P→Pd), −16.84 (1 P, m, P→Pd).

$[Pd_2Co(CO)_4(dppm)_2][PF_6]$ (7). The following reactions and manipulations were performed under a CO atmosphere. A solution of $TlPF_6$ (0.073 g, 0.209 mmol) in acetone (5 mL) was added to a solution of **5** (0.262 g, 0.209 mmol) in CO-saturated acetone (50 mL). An immediate color change from red-brown to orange occurred upon mixing. Stirring and CO bubbling were maintained for 0.5 h. The insoluble TlI was removed by filtration of the solution through a Celite-padded filter funnel (medium porosity). Addition of *n*-hexane to the solution induced precipitation of light red, air-stable, solvated crystals of **7** (0.210 g, 74% based on Pd) (mp 198 °C dec). Anal. Calcd for $7 \cdot C_3H_6O$ ($C_{57}H_{50}CoF_6O_5P_5Pd_2$) ($M_r$ = 1355.66): C, 50.50; H, 3.72. Found: C, 50.38; H, 3.87. IR (KBr) ν(CO) 2072 (s), 2007 (s), 1896 (m, br), ν(PF) 838 (vs) cm^{-1}. IR (THF): ν(CO) 2078 (s), 2013 (s), 1897 (m, br) cm^{-1}. ^1H NMR ($CDCl_3$): δ 7.68–6.88 (40 H, m, C_6H_5), 4.72 (2 H, dt, ^2J(PH) = 9.8 Hz, ^4J(PH) = 2.0 Hz, CH_2), 4.35 (2 H, t, ^2J(PH) = 10.2 Hz, CH_2). $^{31}P\{^1H\}$ NMR ($CH_2Cl_2/CDCl_3$): δ 22.4 (1 P, br m, P→Co), −6.17 (1 P, m, P→Pd), −7.97 (1 P, m, P→Pd), −13.38 (1 P, m, P→Pd).

Decarbonylation–Carbonylation Experiments. When a solution of **7** in THF was evaporated to dryness, it afforded a brown residue **8** whose IR spectrum (THF) exhibited ν(CO) vibrations bands at 2000 (s) and 1879 (m, br) cm^{-1}. The IR spectrum recorded in KBr pellet was that of **4**. Bubbling CO into the THF solution of **8** immediately caused the lightening of the solution and the reappearance of the ν(CO) band at 2078 cm^{-1}, characteristic of **7**. Numerous such cycles were performed without noticeable decomposition. Similar observations were made when acetone, MeCN, or CH_2Cl_2 were used as solvents.

C. X-ray Data Collections and Structural Determinations for $1 \cdot 2.5THF$ and $7 \cdot Me_2CO$. Well-formed prismatic green single crystals of $1 \cdot 2.5THF$ were obtained by slow diffusion of pentane into a THF solution of the complex at −20 °C. Parallelepipedic red single crystals of **7**·Me_2CO were grown from acetone/hexane at room temperature. The structure of **1** was determined by J.F. and that of **7** by S.-E.B. and D.G. Cell constants and other pertinent crystal data are collected in Table II. For **1**, a systematic search in the reciprocal space using a Philips PW 1100/16 automatic diffractometer showed that the crystals belong to the triclinic system. Precise lattice parameters were obtained and refined at room temperature with Cu Kα_1 radiation by using 25 carefully selected reflections and the standard Philips software. The single crystal was sealed in a Lindemann glass capillary and mounted on a rotation-free goniometer head. Intensity data were collected and transferred to a PDP 11/60 computer and the structure was refined by using the SDP/VAX. Three standard reflections measured every hour during the entire data collection period had a mean loss of 11% in intensity, which was corrected by using a time-dependent linear interpolation function. The raw step-scan data were converted to intensities by using the Lehmann and Larsen method[79] and then corrected for Lorentz, polarization, and absorption factors, the latter computed by interpolation of absorption tables.[80] The structure was solved by using the heavy-atom method in space group $P\bar{1}$, assumed on the basis of a $N(z)$ cumulative test on $|F_o|$. After refinement of the heavy atoms, a difference Fourier map revealed maxima of residual electronic density close to the position expected for hydrogen atoms. They were introduced by their computed coordinates (C–H = 0.95 Å) in structure factor calculations with isotropic thermal parameters of 8.0 Å^2, but were not refined. Full least-squares refinements minimizing the function $\sum w(|F_o| - |F_c|)^2$ converged to the R values given in Table II. Each reflection was weighted with $\sigma^2(F_o) = \sigma_{\text{counts}}^2 + (pI)^2$. A final difference map revealed no significant residual peaks. The neutral-atom scattering factors used for all atoms and anomalous dispersion coefficients were obtained from standard sources.[81] For **7**, precise lattice parameters were obtained by standard Enraf-Nonius least-squares methods[78] using 25 carefully selected reflections and Mo Kα radiation. Special attention was paid to the *Cc* space group. No intensity decay was observed during the data collection period. For all subsequent computations the Enraf-Nonius SDP/VIP package was used.[78] Intensities were corrected as for **1** except that absorption corrections were omitted. The crystal structure was solved by using the Multan program[82] and refined as for **1** except that isotropic thermal parameters of 5.0 Å^2 were chosen for the hydrogen atoms. The final difference map showed no significant residual peaks. For **1** and **7**, refinement results are given in Table II and atomic coordinates with estimated standard deviations corresponding to the final least-squares refinement cycles are given in Tables III and IV, respectively. Anisotropic thermal parameters for all non-hydrogen atoms (Tables S-I and S-VII), hydrogen atom coordinates (Tables S-II and S-VIII) and a listing of the observed and calculated structure factor amplitudes used in the refinement (Tables S-VI and S-XI) are available for **1**·$2.5C_4H_8O$ and **7**·C_3H_6O, respectively, as supplementary material.[83]

Acknowledgment. We are grateful to the CNRS for financial support and for a grant to M.R., and we also thank Johnson Matthey Technology Center for a generous loan of $PdCl_2$.

Registry No. **1**, 113109-24-3; **1**·2.5THF, 113109-33-4; **2**, 113109-25-4; **3**, 113109-26-5; **4**, 113109-27-6; **5**, 113109-28-7; **6**, 113109-29-8; **7**, 113109-35-6; **7**·Me_2CO, 113109-36-7; **8** (S = THF), 113109-31-2; $[Pd_2Cl_2(\mu\text{-}CH_2)(dppm)_2]$, 78274-94-9; $Na[Co(CO)_4]$, 14878-28-5; $[Pd_2Cl_2(dppm)_2]$, 64345-29-5; $[Pd_2Cl_2(\mu\text{-}CO)(dppm)_2]$, 64345-32-0; NaF, 7681-49-4; NaCl, 7647-14-5; Pd, 7440-05-3; Co, 7440-48-4; diazomethane, 334-88-3.

Supplementary Material Available: For **1**·$2.5C_4H_8O$ and **7**·C_3H_6O, respectively, tables of anisotropic thermal parameters (Tables S-I and S-VII), calculated hydrogen atom coordinates (Tables S-II and S-VIII), complete bond lengths and angles (Tables S-III, S-IV, S-IX, and S-X), and selected weighted least-squares planes (Table S-V) and a top view of the molecular structure of **1**·$2.5C_4H_8O$ (Figure 3) and infrared spectra in the ν(CO) region (recorded in KBr) of compounds **1**, **3**, and **7** (Figure 4) (27 pages); listings of observed and calculated structure factors (Tables S-VI and S-XI) (49 pages). Ordering information is given on any current masthead page.

---

(78) Frenz, B. A. In *Computing in Crystallography*; Schenk, H., Olthof-Hazekamp, R., van Koningsveld, H., Bassi, G. S., Eds.; University Press: Delft, The Netherlands, 1978; p 64.

(79) Lehmann, M. S.; Larsen, F. K. *Acta Crystallogr., Sect. A: Cryst. Phys., Diffr., Theor. Gen. Crystallogr.* **1974**, *A30*, 580.

(80) *International Tables for X-Ray Crystallography*; Kynoch: Birmingham, England, 1959; Vol. II, p 302.

(81) Cromer, D. T.; Waber, J. T. *International Tables for X-Ray Crystallography*; Kynoch: Birmingham, England, 1974; Vol. IV, Table 2-2b. (b) Cromer, D. T. *Ibid.*, Table 2.3.1.

(82) Germain, G.; Main, P.; Woolfson, M. M. *Acta Crystallogr., Sect. A: Cryst. Phys., Diffr., Theor. Gen. Crystallogr.* **1971**, *A27*, 368.

(83) See paragraph at the end of the paper regarding supplementary material.